UNCLASSIFIED
SECURITY CLASSIFICATION OF THIS PAGE

AD-A214 928

REPORT DOCUMENTATION PAGE

DTIC ELECTE NOV 29 1989 S D

1a REPORT SECURITY CLASSIFICATION: UNCLASSIFIED

1b RESTRICTIVE MARKINGS:

2a SECURITY CLASSIFICATION AUTHORITY:

2b DECLASSIFICATION / DOWNGRADING SCHEDULE:

3 DISTRIBUTION / AVAILABILITY OF REPORT: Approved for public release; distribution is unlimited.

4 PERFORMING ORGANIZATION REPORT NUMBER(S):

5 MONITORING ORGANIZATION REPORT NUMBER(S): AFOSR-TR- 89-1422

6a NAME OF PERFORMING ORGANIZATION: Colorado State University

6b OFFICE SYMBOL (If applicable):

7a NAME OF MONITORING ORGANIZATION: AFOSR/NP

6c ADDRESS (City, State, and ZIP Code): Fort Collins, CO 80523

7b ADDRESS (City, State, and ZIP Code): Building 410, Bolling AFB DC 20332-6448

8a NAME OF FUNDING/SPONSORING ORGANIZATION: AFOSR

8b OFFICE SYMBOL (If applicable): NP

9 PROCUREMENT INSTRUMENT IDENTIFICATION NUMBER: AFOSR-87-0290

8c ADDRESS (City, State, and ZIP Code): Building 410, Bolling AFB DC 20332-6448

10 SOURCE OF FUNDING NUMBERS

PROGRAM ELEMENT NO.	PROJECT NO.	TASK NO.	WORK UNIT ACCESSION NO.
61102F	2301	A1	

11 TITLE (Include Security Classification): (U) CW ULTRAVIOLET LASER EXCITED WITH AN ELECTRON BEAM

12 PERSONAL AUTHOR(S): Dr Jorge J. Rocca

13a TYPE OF REPORT	13b TIME COVERED	14. DATE OF REPORT (Year, Month, Day)	15 PAGE COUNT
Final	FROM 1 Jul 87 TO 30 Jun 89	October 1989	43

16 SUPPLEMENTARY NOTATION:

17 COSATI CODES

FIELD	GROUP	SUB-GROUP
	20.06	

18 SUBJECT TERMS (Continue on reverse if necessary and identify by block number):

19 ABSTRACT (Continue on reverse if necessary and identify by block number)

Laser oscillation was obtained in the 318 nm transition of AgII. Excitation of the laser upper level occurs by charge transfer collisions between ground state neon ions created by electron beam ionization and silver atoms. CW laser oscillation was also obtained in the 478.8 nm line of AgII.

89 11 27 090

20 DISTRIBUTION / AVAILABILITY OF ABSTRACT: [X] UNCLASSIFIED/UNLIMITED [X] SAME AS RPT [ ] DTIC USERS

21 ABSTRACT SECURITY CLASSIFICATION: UNCLASSIFIED

22a NAME OF RESPONSIBLE INDIVIDUAL: H R Schlossberg

22b TELEPHONE (Include Area Code): 202/767-4906

22c OFFICE SYMBOL: AFOSR/NP

DD FORM 1473, 84 MAR — 83 APR edition may be used until exhausted. All other editions are obsolete.

SECURITY CLASSIFICATION OF THIS PAGE
UNCLASSIFIED

AFOSR-TR- 89-1422

CW Ultraviolet Laser Excited with an Electron Beam

AFOSR Grant # 87-0290

Final report for the period July 1, 1988 to June 30, 1989.

Principle Investigator: Dr. Jorge J. Rocca

Institution: Colorado State University

Department: Electrical Engineering

Address: Colorado State University

Fort Collins, Co 80523

Project Summary

We have obtained CW laser action in the ultraviolet in a silver-neon plasma excited by an electron beam. Laser oscillation was obtained in the 318 nm transition of AgII. Excitation of the laser upper level occurs by charge transfer collisions between ground state neon ions created by electron beam ionization and silver atoms. CW laser oscillation was also obtained in the 478.8 nm line of AgII.

These results were obtained operating high voltage glow discharge electron guns in a neon atmosphere for the first time. Previously, electron beam excited CW lasers were limited to the use of helium as the major atomic component of the gain medium. The successful use of neon significantly increases the number of possible laser lines that might be excited by means of selective energy transfer processes involving quasi-resonant collisions. Of particular interest are the CuII laser lines in the vicinity of 260 nm.

Laser output powers of 60 mW and 14 mW were obtained in the visible and ultraviolet transitions of AgII respectively using non-optimized optical cavities. These results were obtained making use of only approximately 20 percent of the volume of the electron beam created plasma to generate the laser radiation. A significant increase in the laser output power could be obtained by optimizing the overlap between the mode volume and the electron beam plasma volume. No saturation of the laser output power with discharge

current was observed up to the maximum current investigated which was 1.45 A. A more complete description of the experiments is given in appendix 1.

In summary, we have developed a CW electron beam laser capable of oscillating in transitions corresponding to elements requiring high vaporization temperatures. CW laser oscillation was demonstrated at 478.8 and at 318 nm in singly ionized silver in a Ag-Ne plasma. This is the first time that electron beam excitation has been successfully used to pump a CW ultraviolet laser. Substitution of the silver by copper is expected to result in CW laser action in the 248-270 nm region.

During the period of this grant, we also extended out study of laser action in the flowing negative glow plasmas. In this scheme, energetic electrons produce a negative glow plasma in a localized region. This plasma is then expanded by a fast gas flow to form a plasma plume in which the plasma ions recombine with cool electrons to excite laser transitions. The separation of the excitation region from the recombination region allows us to obtain CW laser action in atomic and ionic systems in which the excitation of the lower level would forbid the generation of population inversions in the presence of energetic electrons. Previously using this device we demonstrated CW laser action by three-body electron-ion recombination in infrared lines in CdI. We have extended CW laser operation to ArI and have also obtained pulse laser operation of infrared lines of PbI, PbII, ZnI, SnII, H_2, ArI and NeI. The dependence of the laser intensity as a function of the discharge parameters and position of the recombining plasma plume was studied in ArI, PbI, PbII, ZnI and SnII. We also demonstrated that the addition of hydrogen aids plasma cooling and significantly increases the laser intensity. The results of our study are summarized in appendix 2.

Appendix 1

CW Ultraviolet and Visible Laser Action from Ionized Silver in an Electron Beam Generated Plasma

B. Wernsman, J. J. Rocca[a] and H. L. Mancini

Electrical Engineering Department

Colorado State University

Fort Collins, CO 80523

Continuous wave Laser oscillation was obtained in the 318.1 nm and the 478.8 nm lines of AgII in a neon-silver vapor mixture excited by glow discharge electron beams. Laser output powers of 14 mW and 60 mW were obtained in the ultraviolet and blue transitions respectively using non-optimized optical cavities.

a) National Science Foundation Presidential Young Investigator

Previously, we reported laser action in more than 50 ionic and atomic laser lines using electron beam excitation of helium-metal vapor plasmas [1-5]. Different population inversion mechanisms including charge transfer [1,2], collisional electron-ion recombination [3], penning ionization [4] and dissociative excitation [5] have been successfully used to obtain laser oscillation in plasmas generated by glow discharge electron beams. DC electron beam excitation has been demonstrated to produce high CW laser powers as 1.2 W was obtained in the blue lines of ZnII [1]. However up to date CW laser action by electron beam excitation was limited to the infrared and the visible regions of the spectrum and to the use of helium as the major atomic component of the gain medium. Herein we report the operation of a CW electron beam pumped laser in the ultraviolet for the first time. Also we have demonstrated the use of neon as a buffer gas thereby significantly increasing the number of possible laser lines that might be excited with this type of excitation by means of selective energy transfer processes involving quasi-resonant collisions [6].

CW laser action was obtained in the 318.1 nm [$5s^2\ {}^1G_4$ - $5p\ {}^3F_3{}^o$] and the 478.8 nm [$5s^2\ {}^1D_2$ - $5p\ {}^1P_1{}^o$] lines of AgII in a neon-silver plasma excited by a multikilovolt dc electron beam. The laser upper levels are populated by charge transfer collisions between ground state neon ions and ground state silver atoms as previously observed to occur in hollow cathode discharges [7]. The majority of the neon ions are created by electron impact ionization as a consequence of the collisions between high energy electrons and neon atoms.

The laser setup employed in the experiments is similar to that recently used to obtain laser action in the infrared in a He-Ag mixture, and it has been described in detail in a previous publication [2]. The laser active medium is a neon-silver plasma generated inside a molybdenum tube 90 cm in length with an inside diameter of 0.9 cm by the excitation produced by two glow discharge electron guns. A compact tantalum ribbon heater surrounds the plasma tube and produces the necessary temperature to vaporize silver and obtain the metal vapor density required for laser operation. The plasma tube and the heater are placed on the axis of an electromagnet that produces a magnetic field with the purpose of guiding and confining the electron beam. The magnetic field minimizes the scattering of energetic beam electrons to the walls of the plasma tube and consequently allows for a more efficient deposition of the electron beam energy into the plasma. An electron beam is injected into the plasma tube from each end using two electron guns connected to the same dc power supply through separate ballast resistors. The use of a pair of electron guns instead of one allows for the generation of two counter-propogating electron beams which produce a more uniform plasma and increases the available pumping power. The electron guns, which have a 0.5 cm diameter hole through their axis to allow the passage of laser radiation, are constructed using molybdenum-magnesium oxide sintered cathodes that can produce high current dc electron beams in an oxygen free atmosphere [8,9]. The beam electrons are emitted following ion bombardment of a cathode area that is 2.6 cm in diameter.

A small neon flow is maintained through the electron gun chambers which are placed at each end of the plasma tube. Neon is introduced through two independently controlled needle valves and is circulated by a rotary pump. A small pressure difference (0.1 Torr) is maintained between both chambers to establish a small gas flow through the plasma tube with the purpose of obtaining a more even distribution of silver vapor in the entire medium. For all practical purposes the silver vapor is confined to the inside of the plasma tube, and the electron guns which are placed 16 cm from the ends of the plasma tube operate in a pure neon atmosphere.

The current-voltage characteristics of the high voltage neon glow discharge that produces the electron beams differs from those for the helium discharges used in previous experiments. This is a consequence of the difference in the ionization cross-section, ionization energy and ionic mobility of both gases [10]. The I-V characteristics of the high voltage neon glow discharge are illustrated in figure 1. The data was obtained operating the two electron guns simultaneously in the presence of a magnetic field as is done for laser operation. The electromagnet current was adjusted to produce a magnetic field of 3.07 kG in the center of the plasma tube. At 16 cm from the ends of the plasma tube where the emitting surfaces of the electron guns are located, the corresponding value of the magnetic field was measured to be 27 Gauss.

Figure 2a illustrates the variation of the laser output power of the 478.8 nm line of AgII as a function of the discharge current. The data corresponds to the use of a non-optimized optical cavity constructed with a flat total reflecting mirror and a 5 m radius of curvature output coupling mirror having a transmissivity of 1 % at 478 nm. The discharge current threshold for laser action occurred at 0.78 A, and the CW output power of the blue line increased linearly to a value of 60 mW at the maximum electron beam discharge current investigated, 1.15 A. The heater voltage and current were 64 V and 131 A respectively, and the value of the magnetic field was 2.9 kG. Due to the higher ionization cross-section of neon and the corresponding shorter electron mean-free path for the beam electrons, the operation of the Ne-Ag laser requires lower pressure than the He-Ag infrared laser [2]. The optimum average neon pressure was found to be 1.3 Torr. We note that with the optical cavity and electron gun geometry described above only approximately twenty percent of the total plasma volume is used to generate laser radiation, and an increased laser output power could be obtained by optimizing the overlap between the mode volume and the electron beam plasma volume. The variation of the laser output power as a function of the externally applied magnetic field is illustrated in figure 2b. The dependence is similar to that previously observed for the 840.4 nm line of AgII in a He-Ag mixture [2].

When a cavity was implemented using two high reflecting ultraviolet mirrors, CW laser action was readily obtained in the 318.1 nm line of AgII. Threshold for laser oscillation occurred at 0.55 A, and the laser output power increased linearly without signs of saturation up to the maximum electron beam discharge current investigated, 1.0 A. For comparison when high reflectivity mirrors in the blue were used, the current threshold for laser oscillation in the 478.8 nm line was measured to be similar, 0.44 A. By substituting one of the high reflecting ultraviolet mirrors with an output coupler having a transmissivity of 1.3 % at 318 nm and a radius of curvature of 10 m, a maximum CW laser output power of 14 mW was measured. The dependence of the ultraviolet laser power as a function of electron beam discharge current is shown in figure 3 for a neon pressure of 1.3 Torr. When the neon pressure was lowered to 1 Torr the current threshold for ultraviolet laser oscillation decreased to 0.68 A, but the maximum laser power obtained at this pressure was only 5 mW.

In summary, we have demonstrated the operation of an electron beam excited CW laser in the ultraviolet for the first time, and we have expanded the number of possible laser lines for this type of excitation by demonstrating the use of neon as a buffer gas.

The authors want to thank K. Lewis, T. Prabhuram, M. Villagran and F. Gonzalez for their assistance in the construction and initial testing of the laser device. We also want to thank L. Spinelli and T. Johnston of Coherent Inc. for lending us the mirrors used in these experiments and W. Silfvast for encouraging discussions.

This work was supported by an AFOSR grant #87-0290 and a National Science Foundation Presidential Young Investigators Award to J. J. Rocca. H. L. Mancini acknowledges the support of CONICET, Argentina.

References

1) J. J. Rocca, J. D. Meyer and G. J. Collins, "1-W CW Zn ion laser," *Appl. Phys. Lett.*, vol. 43, pp. 37-39, 1983.

2) B. Wernsman, T. Prabhuram, K. Lewis, F. Gonzalez, M. Villagran and J. J. Rocca, "CW Silver Ion Laser with Electron Beam Excitation," *IEEE J. Quantum Electron.*, vol. QE-24, pp. 1554-1556, 1988.

3) J. J. Rocca, H. L. Mancini and B. Wernsman, "Cd Recombination Laser in a Plasma Generated by an Electron Beam," *IEEE J. Quantum Electron.*, vol. QE-22, pp. 509-512, 1986.

4) J. J. Rocca, J. D. Meyer, Z. Yu, M. Farrell and G. J. Collins, "Multikilowatt Electron Beams for Pumping CW Ion Lasers," *Appl. Phys. Lett.*, vol. 41, pp. 811-813, 1982.

5) J. J. Rocca, J. D. yer, B. G. Philstrom and G. J. Collins, "CW Laser Action in Atomic Florine," *IEEE J. Quantum Electron.*, vol. QE-20, pp. 625-628, 1984.

6) W. R. Bennett, "Atomic Gas Laser Transition Data," IFI/Plenum, New York, 1980.

7) J. R. McNeil, W. L. Johnson, G. J. Collins and K. B. Persson, "Ultraviolet Laser Action in He-Ag and Ne-Ag Mixtures," *Appl. Phys. Lett.*, vol. 29, pp. 172-174, 1976.

8) J. J. Rocca, J. D. Meyer, M. R. Farrell and G. J. Collins, "Glow-Discharge-Created Electron Beams: Cathode Materials, Electron Gun Designs, and Technological Applications," *J. Appl. Phys.*, vol. 56, pp. 790 797, 1984.

9) B. Szapiro and J. J. Rocca, "Electron Emission from Glow-Discharge Cathode Materials due to Neon and Argon Ion

Bombardment," *J. Appl. Phys.*, vol. 65, pp. 3713-3715, 1989.

10) E. W. McDaniel, "Collisional Phenomena in Ionized Gases," J. Wiley and Sons, New York, 1964.

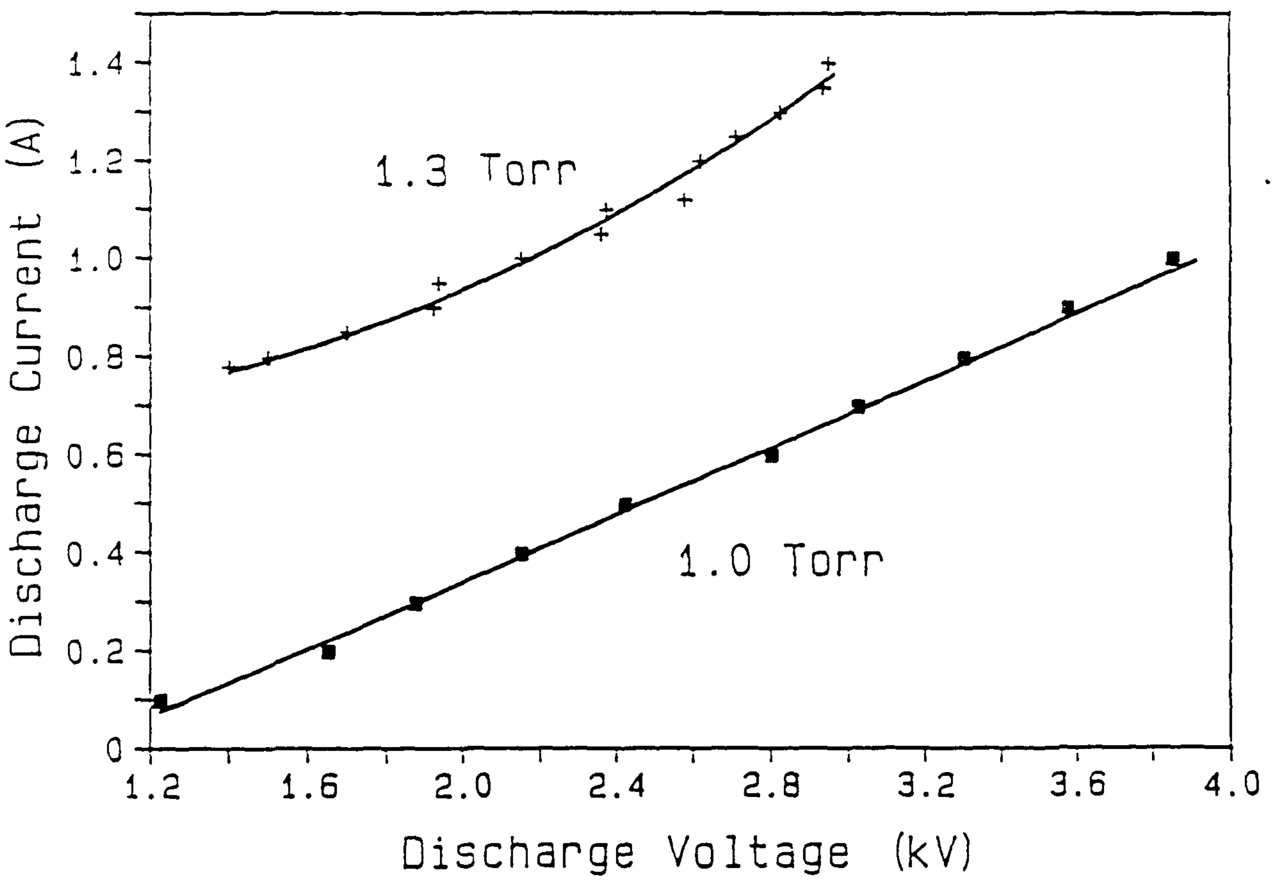
1.3 Torr
1.0 Torr
Discharge Current (A)
Discharge Voltage (kV)
0
0.2
0.4
0.6
0.8
1.0
1.2
1.4
1.2
1.6
2.0
2.4
2.8
3.2
3.6
4.0

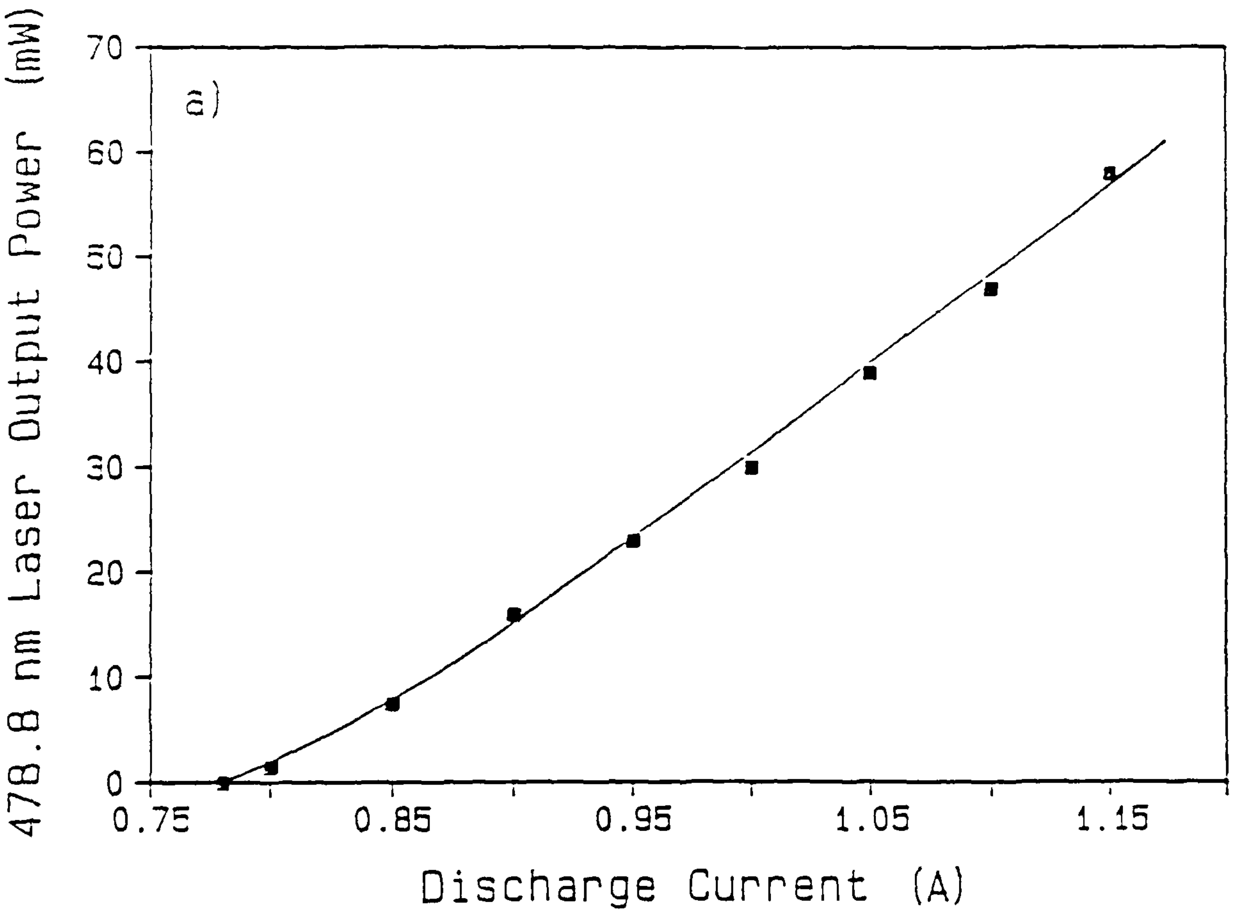

a)
478.8 nm Laser Output Power (mW)
70
60
50
40
30
20
10
0
0.75
0.85
0.95
1.05
1.15
Discharge Current (A)

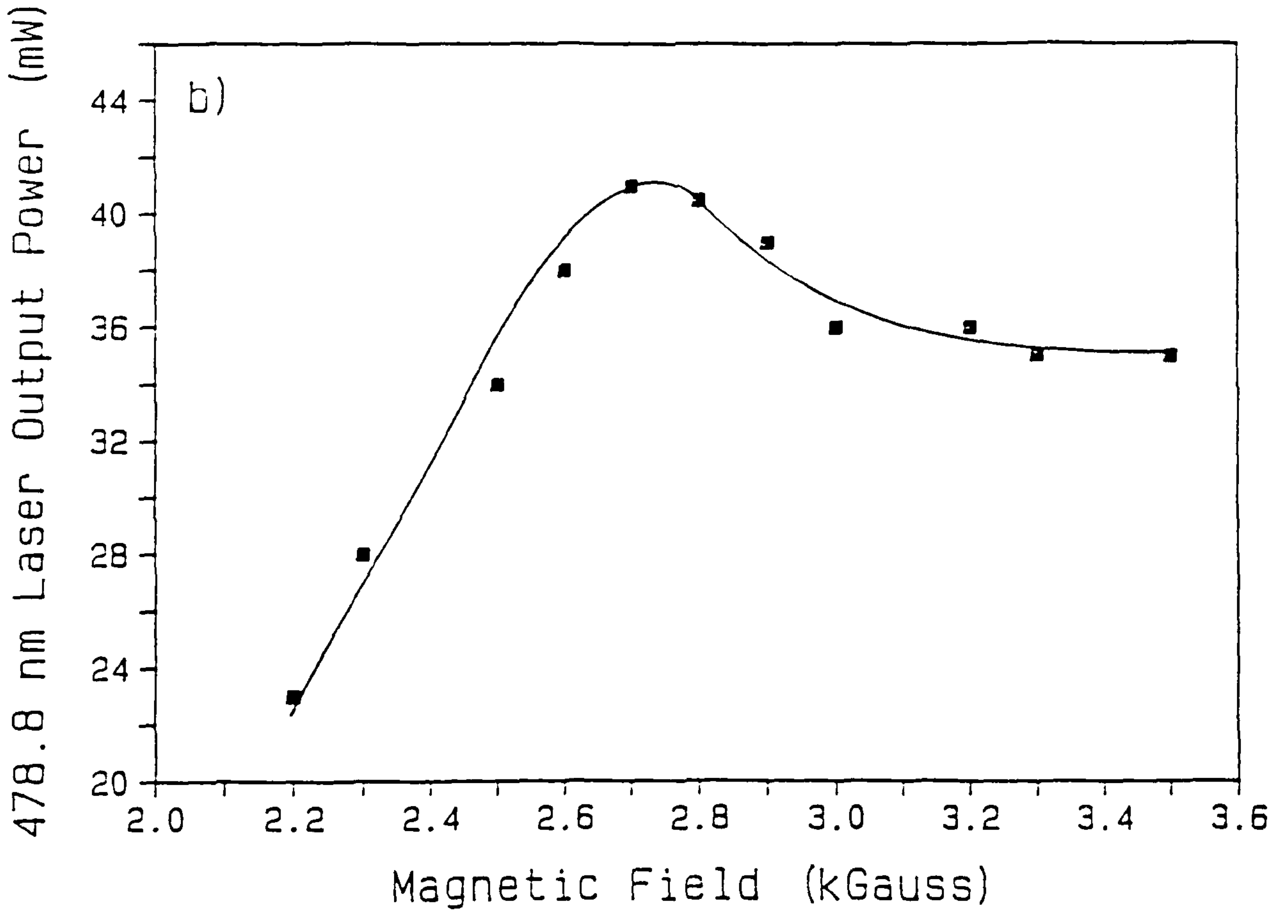
b)
478.8 nm Laser Output Power (mW)
44
40
36
32
28
24
20
2.0
2.2
2.4
2.6
2.8
3.0
3.2
3.4
3.6
Magnetic Field (kGauss)

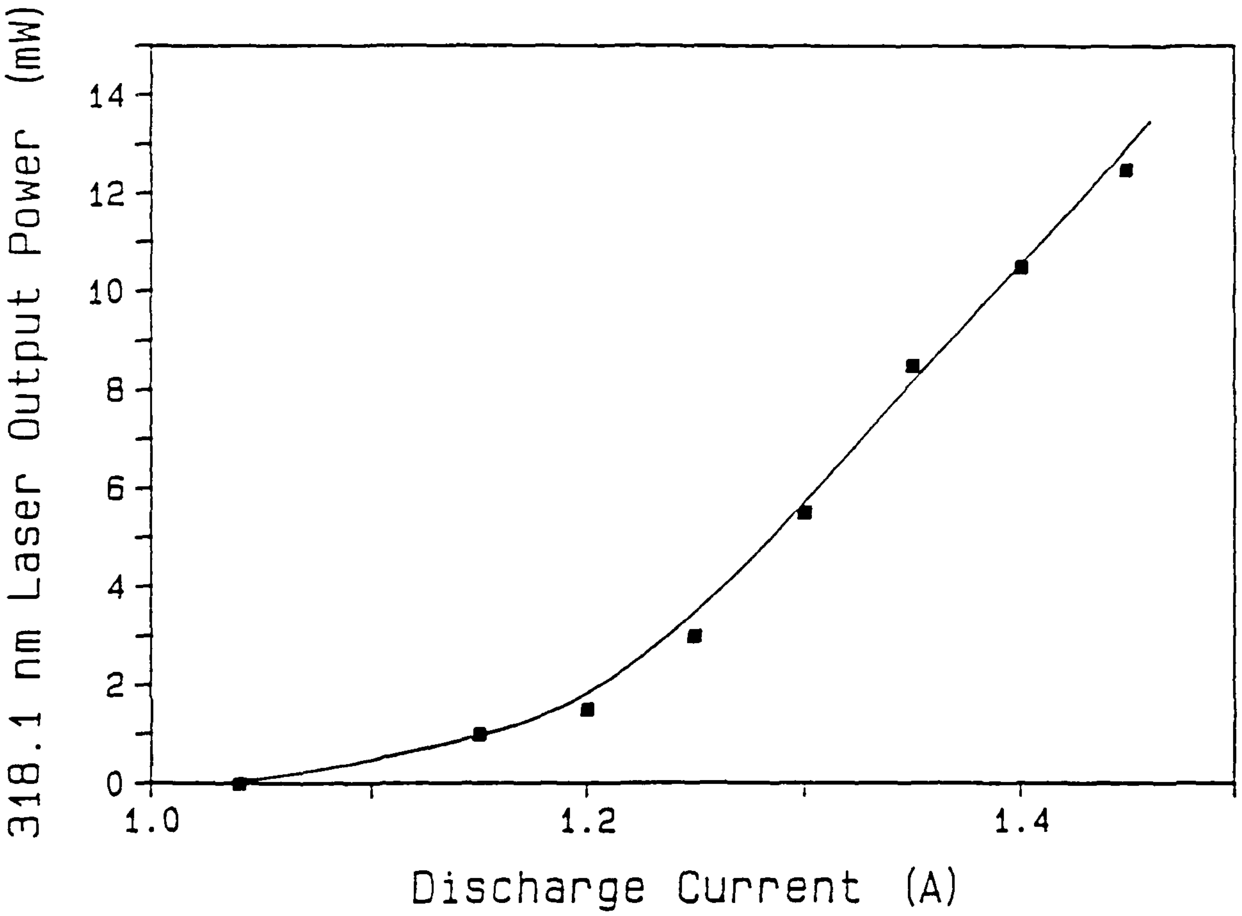

318.1 nm Laser Output Power (mW)
0
2
4
6
8
10
12
14
1.0
1.2
1.4
Discharge Current (A)

Appendix 2

Laser Oscillation in a Flowing Negative Glow Plasma

I. Introduction:

Continuous wave laser oscillation by electron-ion recombination was previously demonstrated by J. J. Rocca in cadmium using a flowing using a flowing negative glow plasma [1]. Negative glow plasmas have an electron energy distribution in which energetic beam electron and supercooled secondary electrons coexist under steady-state conditions and can be advantageously used for the excitation of recombination lasers. The ideal plasma for a recombination laser should have both a large density of energetic electrons for efficient ionization and a large concentration of cool electrons for rapid recombination. By using electron beams, it is possible to generate stationary plasmas that are simultaneously dense and cold. In negative glow plasmas, the ionization is due to energetic beam electrons. Secondary electrons, which result from ionization processes mostly with zero energy, can only gain energy from elastic collisions with beam electrons and in superelastic de-excitation processes. These electrons are thermalized at a low energy by frequent collisions with gas atoms. In stationary negative glow plasmas, the energy of the thermalized electrons is typically 0.1 eV. A fast gas flow is used to create a plasma recombination region without energetic electrons with the purpose of avoiding electrons impact excitation of the laser lower levels, which frequently forbids CW laser oscillation by electron-ion recombination [1].

Herein we discus the use of the same flowing hollow cathode laser system to demonstrate near-infrared laser action in lead, tin, zinc, hydrogen, argon and neon. Continuous wave laser oscillation by collisional electron-ion recombination was observed in argon. Four other collisional recombination laser transitions were observed in a pulsed mode in PbI, PbII, ZnI and SnII. In addition, six other laser transitions excited by other mechanisms were observed in hydrogen, argon, tin and neon.

II. Flowing Hollow Cathode Laser System:

A schematic representation of the flowing hollow cathode laser system used for the excitation of recombination laser action is shown in figure 1. A discharge is established between a hollow cathode and a mesh anode. The cathode has a slot 4 cm long, 1.2 cm deep and 0.2 cm wide. Helium first flows through the anode mesh and then through the cathode slot at a flow rate of 6 liters per minute measured at 760 Torr. Argon or neon is added to enhance cathode sputtering. A rotary pump with a pumping rate of 1000 liters per minute is used to initially evacuate the vacuum chamber to a pressure of 10^{-3} Torr and to establish the gas flow. The gas flow creates a recombining plasma plume downstream of the cathode. The hollow cathode is made of the selected laser material and is soldered into a water cooled copper body. Metal vapor is produced by sputtering of the hollow cathode material. Glow discharges were created using pulsed and dc power excitation. Pulsed currents reaching 35 A with pulsewidths between 10 and 50 μs at a

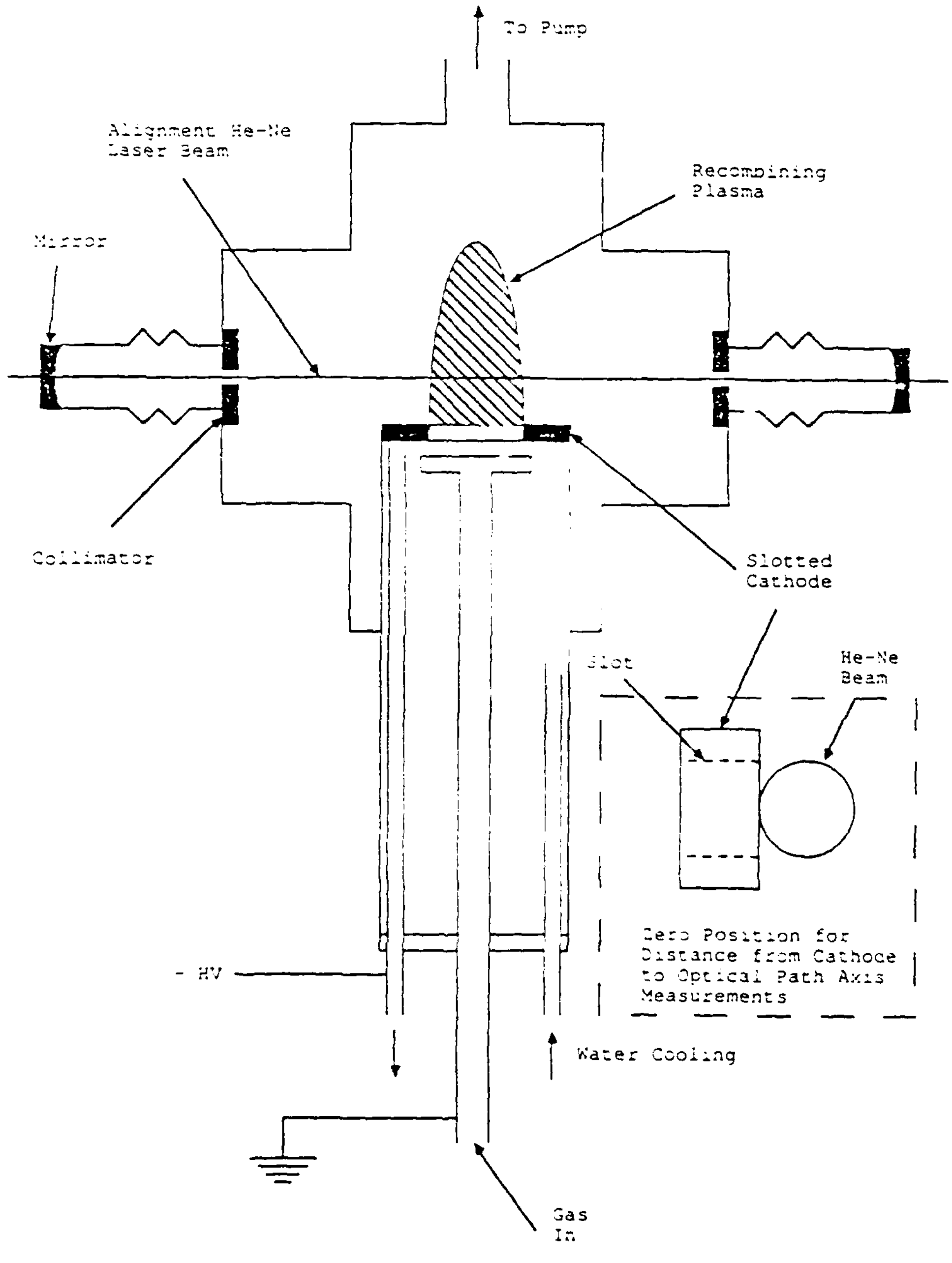

Figure 1: Schematic representation of the flowing hollow cathode laser system. The positioning of the collimators and the setting for the zero point for the measurements of the distance between the cathode and optical path axis are also shown.

frequency of 500 Hz and dc currents up to 2 A were used for the excitation. In the latter case, a 500 Ω series ballast resistance was used. A dense negative glow develops within the cathode slot, and a short positive column links it to the anode. The plasma in the slot is expanded downstream from the gas inlet by the flowing gas to form a stationary low temperature recombining plasma plume as shown in figure 1.

Figure 2 is a picture of the discharge structure showing the anode and slotted cathode. The entire discharge structure is mounted in a glass tube that is movable with respect to the axis of an optical resonator using a dynamic vacuum seal. The ability to move the glass tube allowed the exploration of laser action in different regions of the recombining plasma jet. To make spatially resolved measurements of the emission of the different regions of the recombining plasma plume, two 2 mm diameter collimators were used. The collimators restricted the portion of the recombining plume being observed. Figure 1 also shows the setting of the zero reference for the measurements of the distance from the cathode to the axis of the optical path. The zero reference position is set such that the cathode position is adjusted to touch a helium-neon laser beam centered in the collimators.

The optical cavity for the laser experiments was made of two mirrors each with a 2 meter radius of curvature. Two sets of mirrors were used: one set has a dielectric coating that is highly reflective ($R \geq 99\%$) in the 1.0 - 1.5 μm spectral region, and the other is highly reflective in the 1.5 - 2.0 μm spectral region. The optical cavity was set with its axis in the same plane as the cathode slot. A Ge

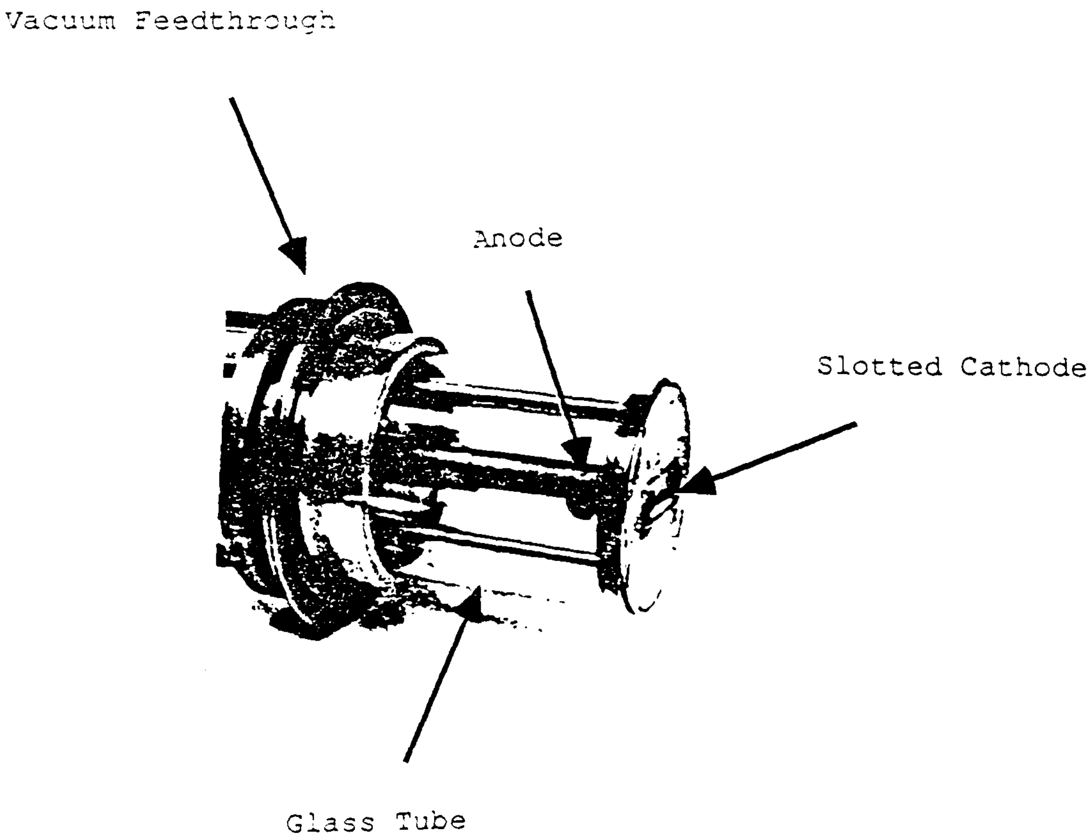

Figure 2: Photograph showing discharge structure of flowing hollow cathode.

photodiode with a rise time of 20 ns was used to detect the laser light that was emitted.

III. Recombination Lasing in Lead:

Two lead laser transitions were observed under pulsed excitation in the flowing afterglow when the slotted cathode was fabricated of lead. The measured laser wavelengths are 13102 ± 2 and 13216 ± 2 Å. The emission is assigned to the 13100.1 Å line of PbI (7p $^3P_1$ - 7s $^3P_1^o$) and the 13216.9 Å line of PbII (6f $^2F_{7/2}^o$ - 7d $^2D_{5/2}$) respectively [2]. W. T. Silfvast, L. H. Szeto and O. R. Wood II reported a PbI transition at 13080 Å and also designated it as the 13100.1 Å transition [3,4], and Zhukov, Latush, Mikhalevskii and Sem previously observed the 13216.9 Å laser transition of PbII [5]. A partial Grotrian diagram showing these two transitions is given in figure 3. The lead transitions did not lase in a CW mode where a dc current up to 2 A was applied.

The output intensity of the PbI and PbII laser lines as a function of distance between the cathode and optical path for two different discharge currents is shown in figure 4. The PbI transition at 13100.1 Å was observed to lase both in a He-Ar mixture and in pure Ar. Based on this fact and from the spatial distribution of the laser output which peaks at 0.5 - 1.0 cm from the cathode depending on the discharge current, it is inferred that the PbI line is an electron-ion recombination excited laser transition.

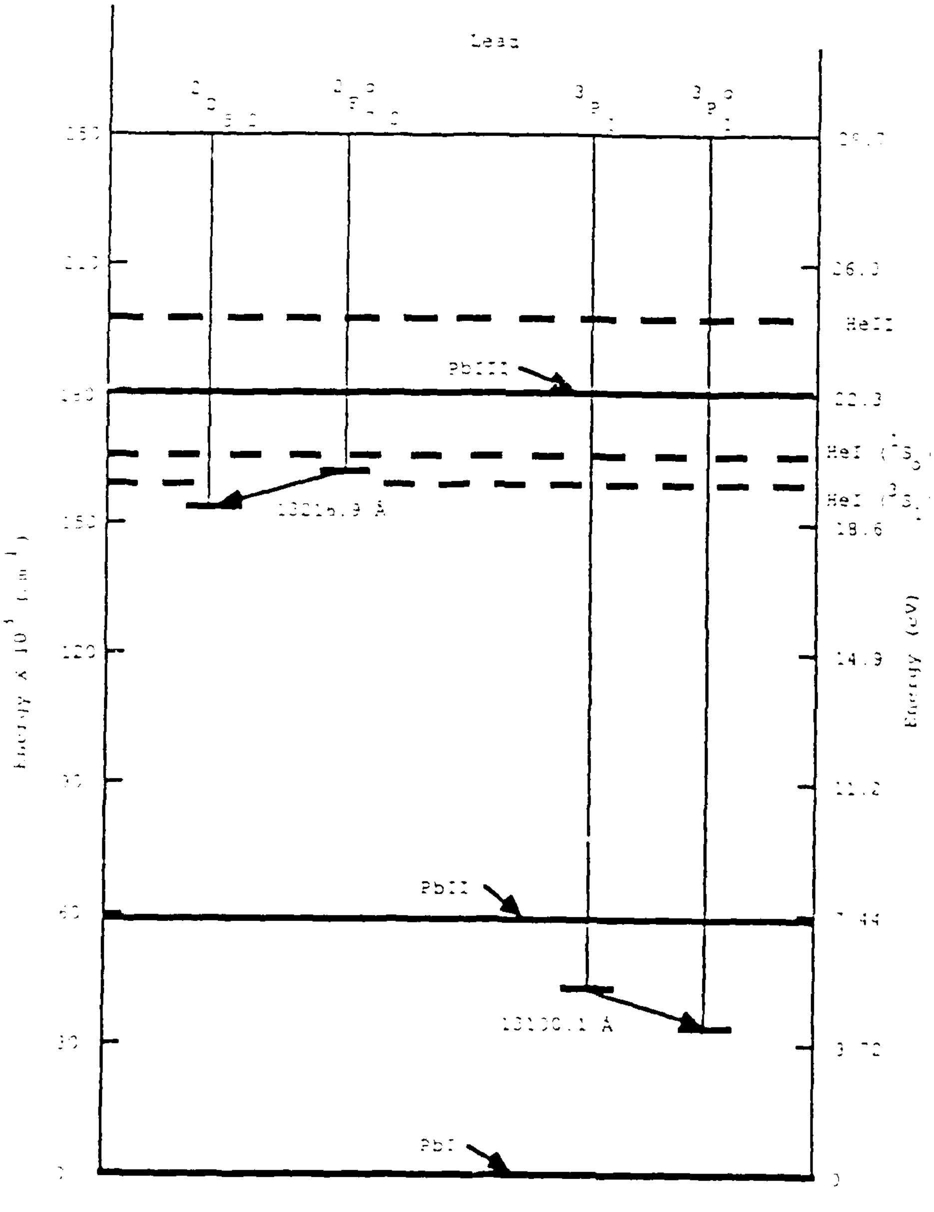

Figure 3: Partial Grotrian diagram of lead.

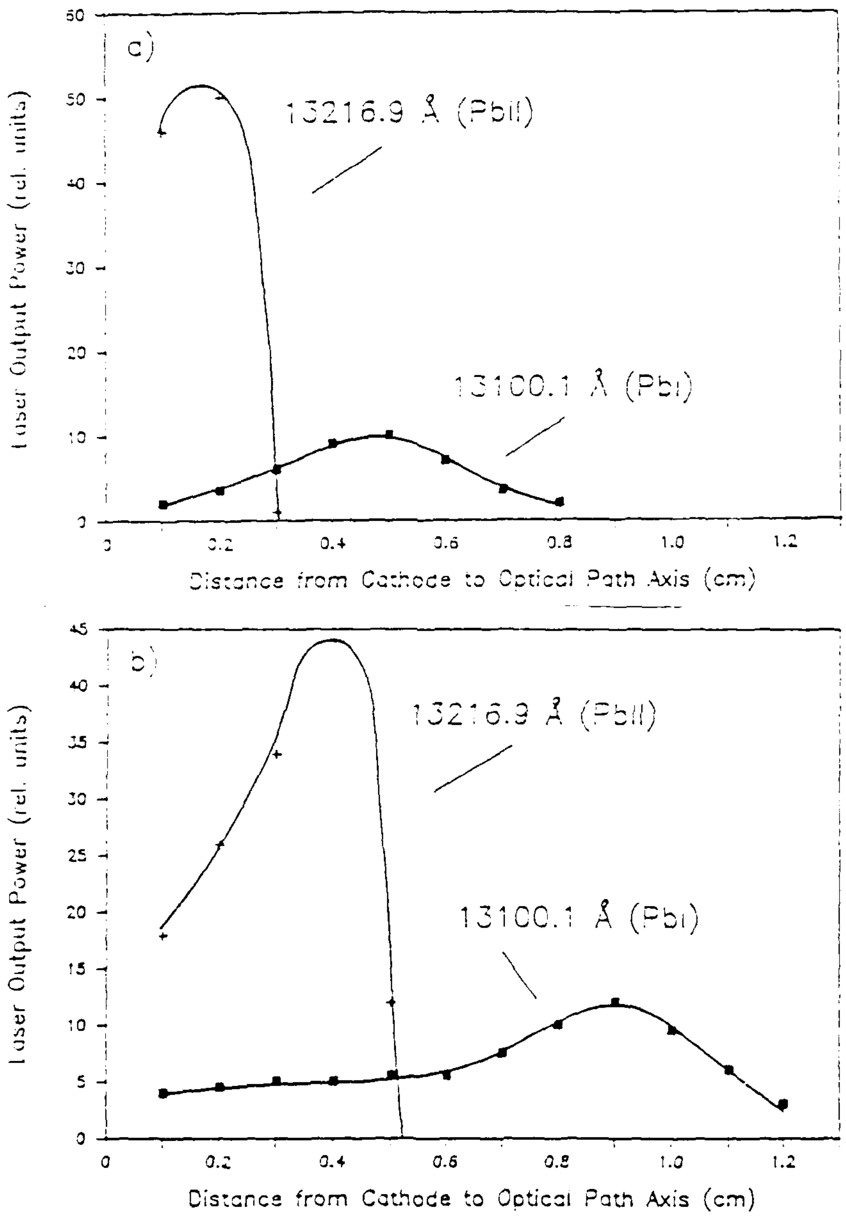

Figure 4: Laser output of the two Pb laser transitions as a function of distance between the cathode and optical path axis. The current pulsewidth was 20 µs. (a) is for a discharge current of 5 A while (b) is for a discharge current of 10 A. Gas flows were 1.3 liters per minute for Ar and 4 liters per minute for He. Two 2 mm diameter collimators were employed for spatial resolution.

As shown in figure 5, the PbI laser transition is thought to be excited by the following manner. First, high energy electrons collide with the helium atoms exciting them to the metastable states of the helium atom and to the ground state of the helium ion. Electron collisions with helium dominate over those with lead since lead is an impurity in the helium buffer gas. A fraction of the helium ions and metastable atoms are driven out of the cathode slot by the gas flow and remain in this state until they collide with the lead atoms transferring their stored energy to the lead atoms through a charge transfer or Penning reaction. These excited lead ions then cascade radiatively and collisionally to the PbII ground state. The PbII ions then undergo three-body electron-ion recombination preferentially populating high lying levels in the lead atoms. These atoms then undergo radiative and collisional de-excitation to the laser upper level where an inversion is created, and laser oscillation can take place.

The PbII laser transition occurs closer to the cathode and is thought to be excited following the recombination of PbIII ground state ions. Zhukov *et. al.* have attributed the excitation of this laser transition in the temporal afterglow of a positive column glow discharge to an electron-ion recombination of the PbIII ground state which is excited by

$$He^{+}(1s\ ^{2}S_{1/2}) + Pb(6p^{2}\ ^{3}P_{0}) \longrightarrow Pb^{++}(6s^{2}\ ^{1}S_{0}) + He(1s^{2}\ ^{1}S_{0}) + e^{-} + \Delta E(2.1\ eV). \quad (1)$$

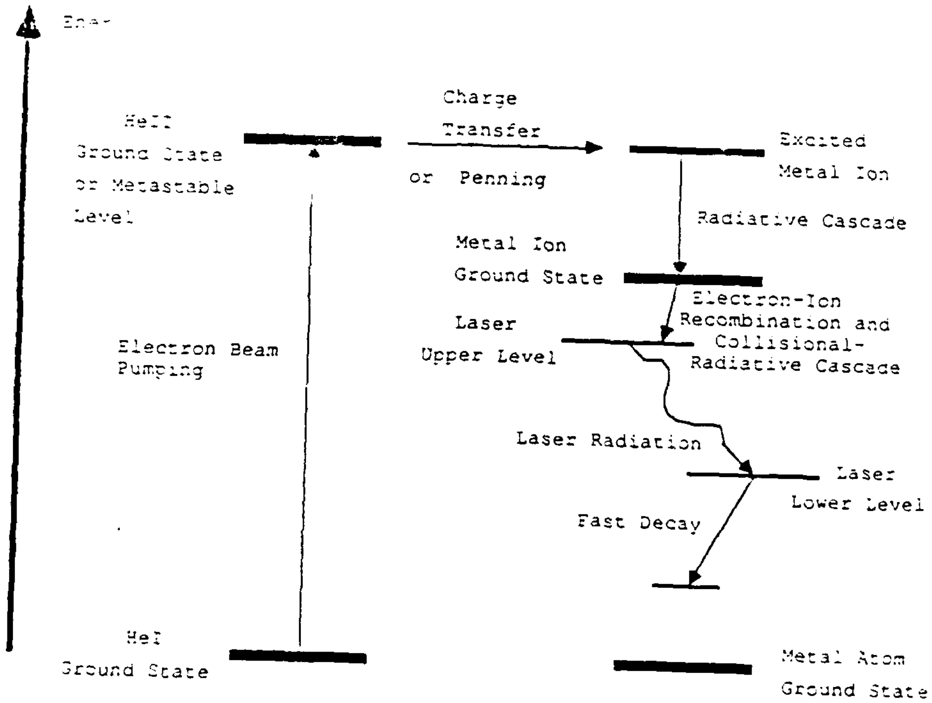

Figure 5: Typical excitation paths in the flowing hollow cathode recombination laser system.

This type of hybrid Duffendack-Penning reaction has been confirmed to occur with high efficiency in a He-Pb afterglow [6]. In a helium afterglow with an ion density of 10^{11} cm^{-3} and a $He_M^*(2s\ ^3S_1)$ density of 10^{10} cm^{-3} the excitation of highly excited states of singly ionized lead was observed to be as strong as the direct excitation of lower lying levels by conventional Penning reactions [6].

A Penning ionization could also contribute to excitation of the PbII laser transition. As shown in figure 3, Penning ionization reaction between the $He_M^*(2s\ ^1S_0)$ metastable state and the ground state lead atoms is energetically allowed:

$$He_M^*(2s\ ^1S_0) + Pb(6p^2\ ^3P_0) \longrightarrow He(1s^2\ ^1S_0) + Pb^{+*}(6f\ ^2F_{7/2}{}^o) + e^- + \Delta E(0.44\ eV). \tag{2}$$

However, the $He_M^*(2s\ ^1S_0)$ population is limited by superelastic electron de-excitation, and in flowing afterglow helium experiments, the only metastable atoms present in quantities detectable by optical absorption are those in the $He_M^*(2s\ ^3S_1)$ level [6]. Never the less, excitation of the laser upper level from the $He_M^*(2s\ ^3S_1)$ is not energetically allowed. Consequently, while Penning excitation probably makes a contribution to the excitation of the $Pb^{+*}(6f\ ^2F_{7/2}{}^o)$ state, recombination from doubly ionized lead is likely to be the dominate excitation path.

The plots of figure 4 also depict that an increase in the excitation current causes the position corresponding to the peak of the laser intensity to move away from the cathode. This dependence is due to a higher electron density at higher currents which increases the superelastic electron de-excitation of the laser upper level for both transitions.

Figure 6 illustrates the laser output and the time delay with respect to the end of the current pulse for both lead laser transitions as a function of the He flow. A constant flow of argon at a rate of 1.1 liters per minute was used. The laser output intensity of the PbI recombination laser transition increased while the time delay decreased as He was added to the flow. This result is probably caused by the more efficient cooling of the plasma which increased the electron-ion recombination. The laser output of the PbII laser transition did not occur until the He flow was greater than the argon flow. This shows that the excitation of this laser transition is helium dependent and eliminates the possibility of direct electron impact excitation of the PbII laser transition. The helium flow at which the PbII transition started to lase was 2.5 liters per minute. The output increased with increased gas flow until the flow was 3 liters per minute. The time delay was simultaneously observed to decrease slightly. This increase in the laser output and decrease in the time delay is attributed to a higher excitation of the laser upper level. The drop in the laser output for a helium flow above 3 liters per minute was accompanied by a slight increase in the time delay. This phenomena is possibly due to a decrease in cathode sputtering. Laser action in the PbI transition was also observed to occur in a pure argon discharge. Figure 7 shows the dependence of the laser intensity of the PbI 13100.1 Å line and its time delay with respect to the end of the current pulse as a function

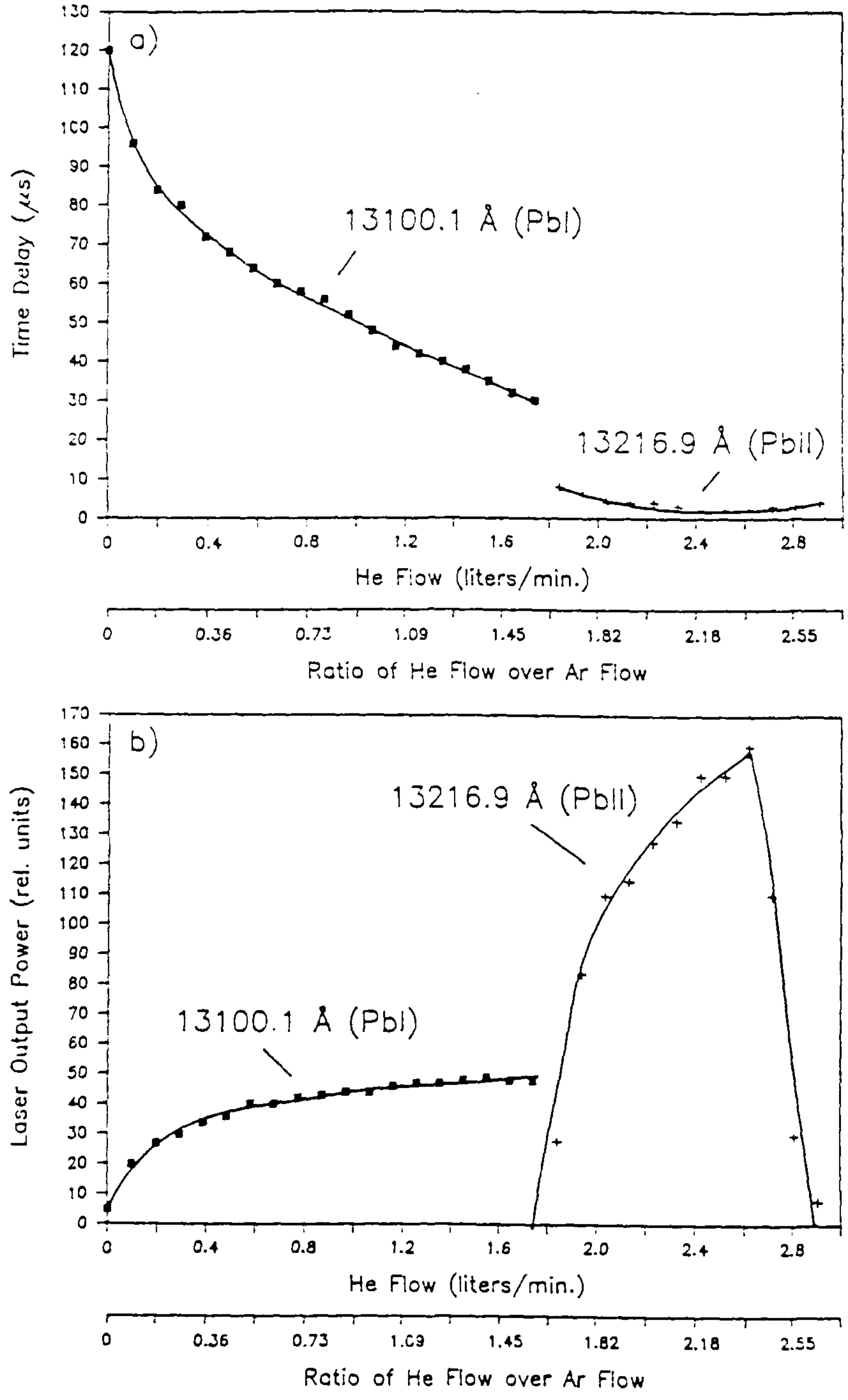

Figure 6: (a) Time delay and (b) laser output intensity for the 13100.1 Å PbI and 13216.9 Å PbII laser transition as a function of He flow. Discharge current was 7 A with a pulsewidth of 30 μs. Ar flow remained constant at 1.1 liters per minute which means it dominates for the first half of the plot. Distance between cathode and optical path axis was 0.1 cm. No collimators were employed.

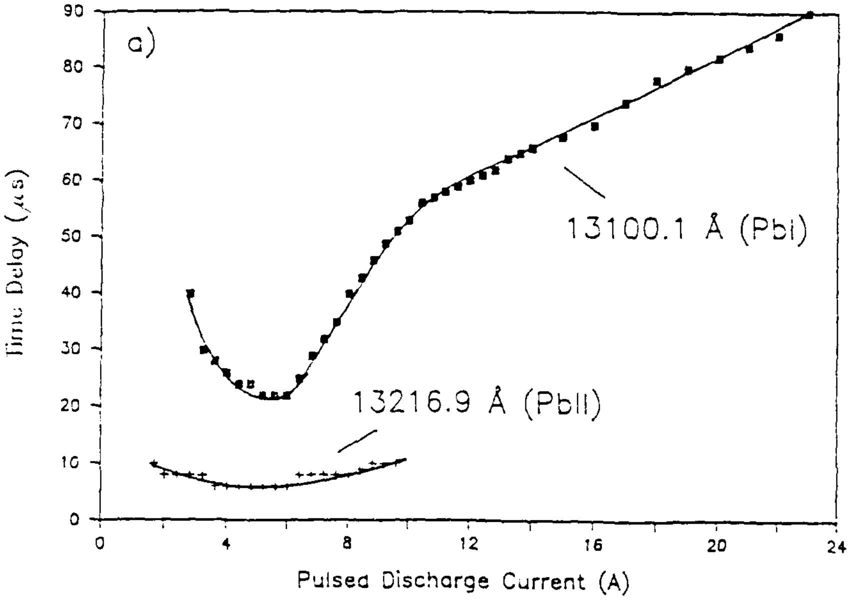

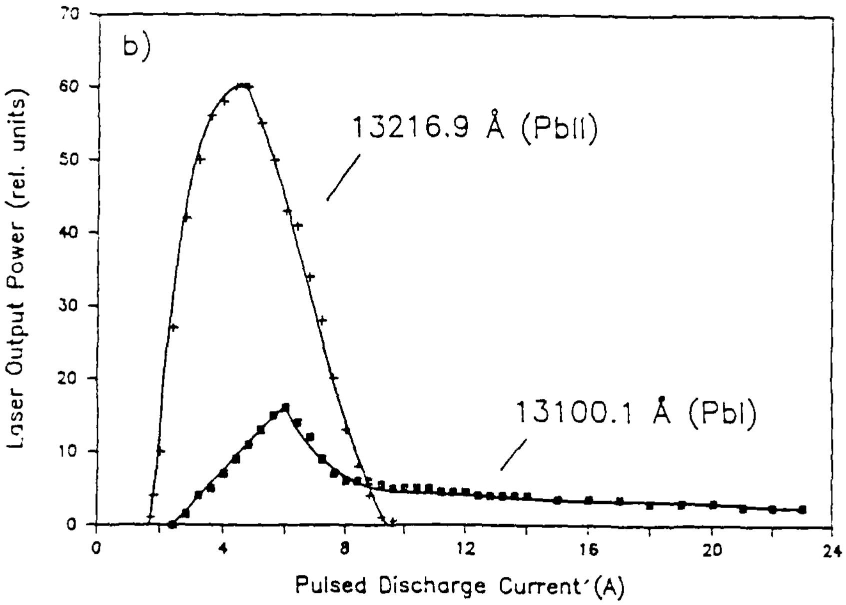

Figure 7: (a) Time delay and (b) laser output intensity for both the 13100.1 Å PbI and 13216.9 Å PbII laser transitions as a function of the discharge current. Current pulsewidths were 30 μs. Distance between cathode and optical path axis for the recombination and Penning excited laser transitions were 0.5 and 0.2 cm, respectively. Gas flows were 1.3 liters per minute for Ar and 4 liters per minute for He. No collimators were used.

of varying argon flow. These plots show that as the argon flow increased the laser output diminished and the time delay increased.

Figure 8 gives the change in the laser output intensity and the time delay between the end of the current pulse and beginning of the laser pulse as a function of discharge current. As shown, the PbI recombination laser transition output increased and the corresponding time delay decreased when the current was increased from the threshold value of 2.8 to 6 A. This increased laser intensity and decreased time delay corresponded to an increase of the electron-ion recombination rate and of the small signal gain with larger currents. However when the input current was increased above 6 A, the laser output decreased and the time delay increased. This behavior is due to the increase in superelastic electron de-excitation of the laser upper level due to a higher electron density.

When the input current changed from its threshold value of 1.7 to 5 A as shown in figure 8, the laser output of the PbII laser transition increased while the time delay decreased slightly. The increased output and diminished time delay are a consequence of a higher pumping rate which increased the number of helium ions and consequently the PbII ions. The decrease of the laser output for discharge currents above 5 A might be due to superelastic electron de-excitation of the laser upper level which diminishes the population inversion. Lead was not observed to lase in the 1.5 - 2.0 μm spectral region.

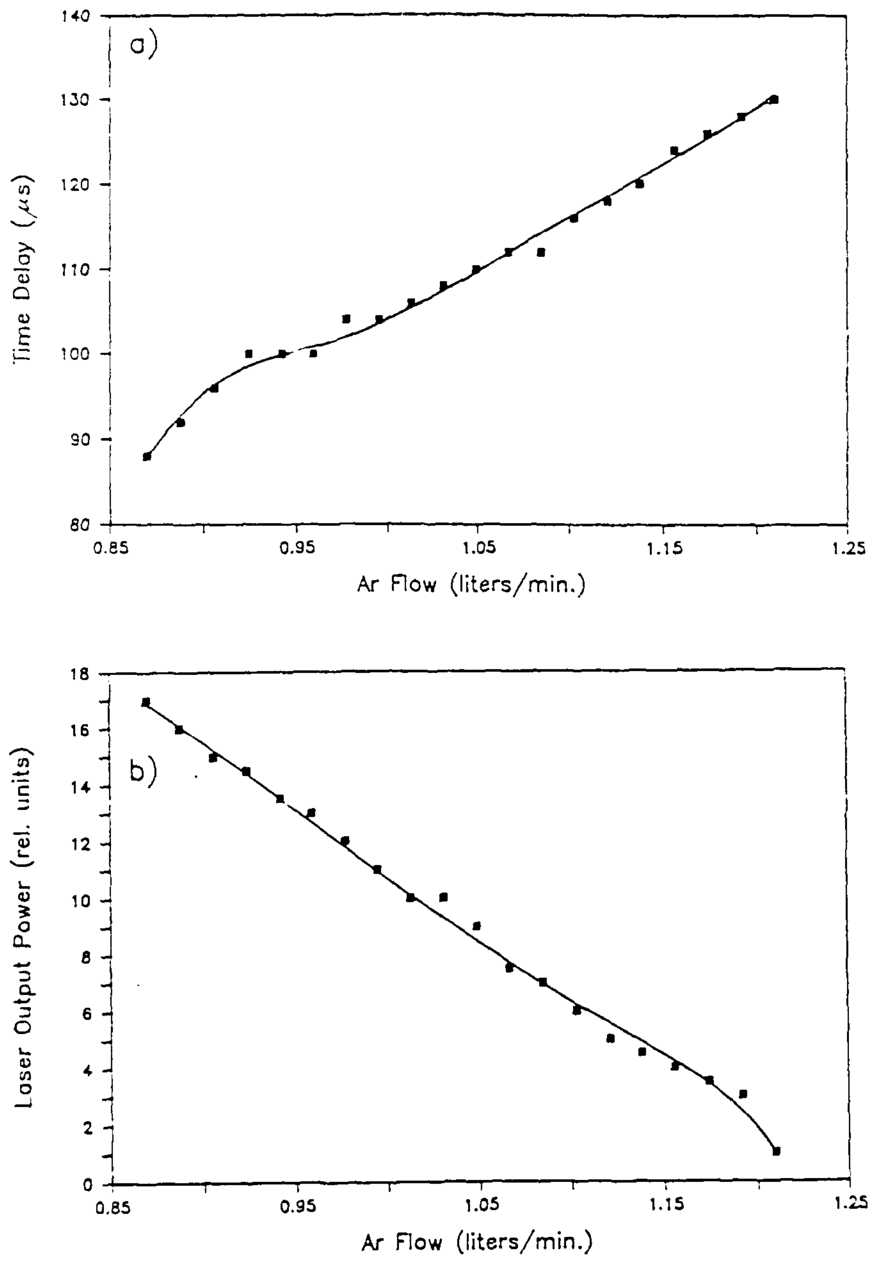

Figure 8: (a) Time delay between the laser pulse and the end of the current pulse, and (b) laser output intensity for the 13100.1 Å PbI laser transition as a function of the Ar flow. Discharge current was 7 A with a pulsewidth of 30 μs. Distance between cathode and optical path axis was 0.1 cm. No collimators were used.

IV. Laser Action in Tin:

Replacing the slotted lead cathode with one made of tin enabled the achievement of an ionic tin laser transition. The measured wavelength of this transition was 10737 $\pm$ 2 Å. The gas flows were 1.3 liters per minute for Ar and 4 liters per minute for He. This line is assigned to the SnII transition of 10738.7 Å (5f $^2F_{5/2}{}^o$ - 6d $^2D_{5/2}$) [2,7]. V. V. Zhukov *et. al.* observed a laser transition in SnII at a wavelength of 10740 Å and assigned it to the 5f $^2F_{7/2}{}^o$ - 6d $^2D_{5/2}$ transition [5,8]. The 5f $^2F_{7/2}{}^o$ - 6d $^2D_{5/2}$ transition corresponds to a wavelength of 10743.3 Å [2,7]. A partial Grotrian diagram of SnII showing this laser transition is given in figure 9.

A plot of the laser output intensity as a function of the distance between the slotted cathode and the optical path axis is given in figure 10. This plot is similar to that of figure 5 corresponding to the PbII laser line.

Zhukov *et. al.* attributed this SnII laser transition observed during the afterglow of a positive column glow discharge to an electron-ion recombination reaction of the SnIII ground state which was excited by the reaction

$$He^+(1s\ ^2S_{1/2}) + Sn(5p^2\ ^3P_0) \longrightarrow Sn^{++}(5s^2\ ^1S_0) + He(1s^2\ ^1S_0) + e^- + \Delta E(2.6\ eV) \qquad (3)$$

as they did for the PbII laser transition.

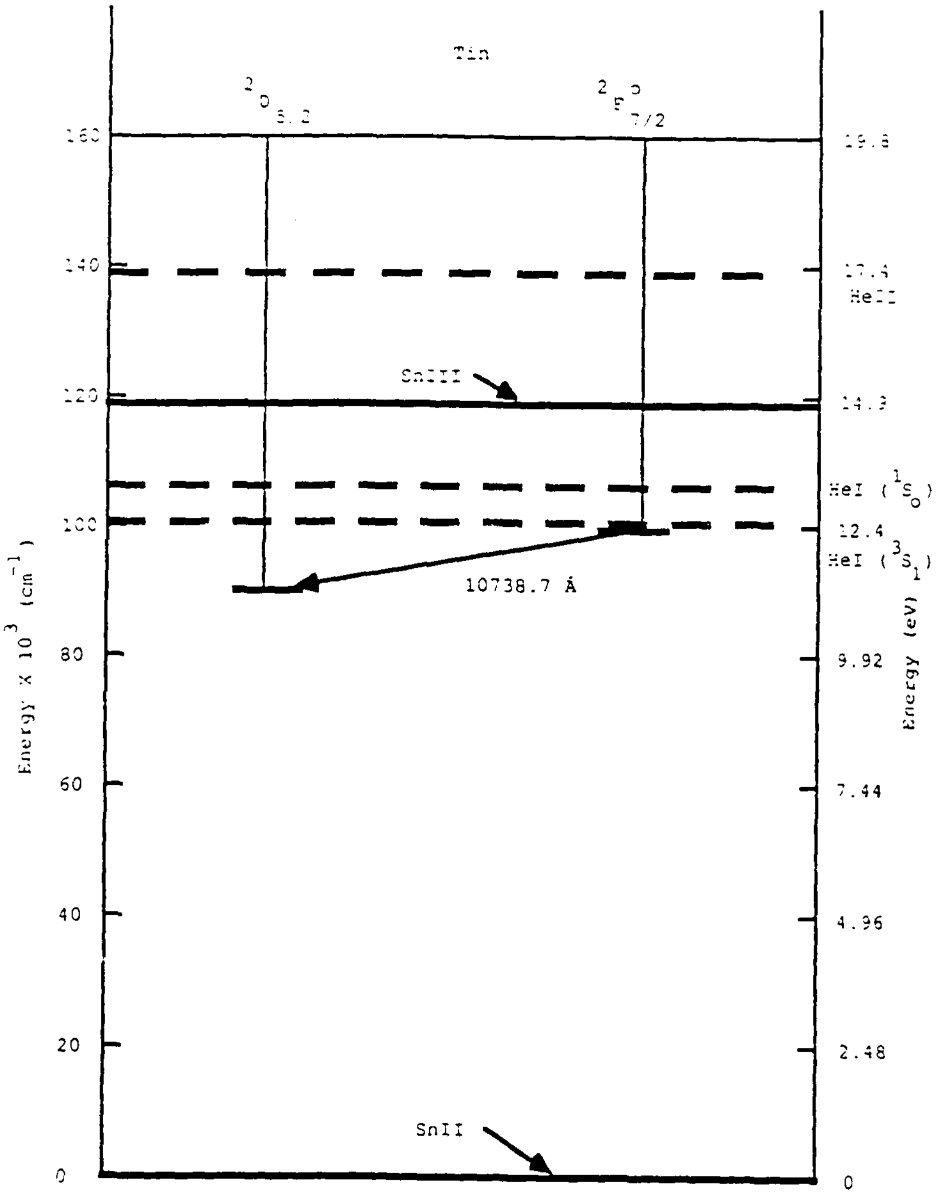

Figure 9: Partial Grotrian diagram of tin. The ionization of SnII is taken as the origin of the energy axis.

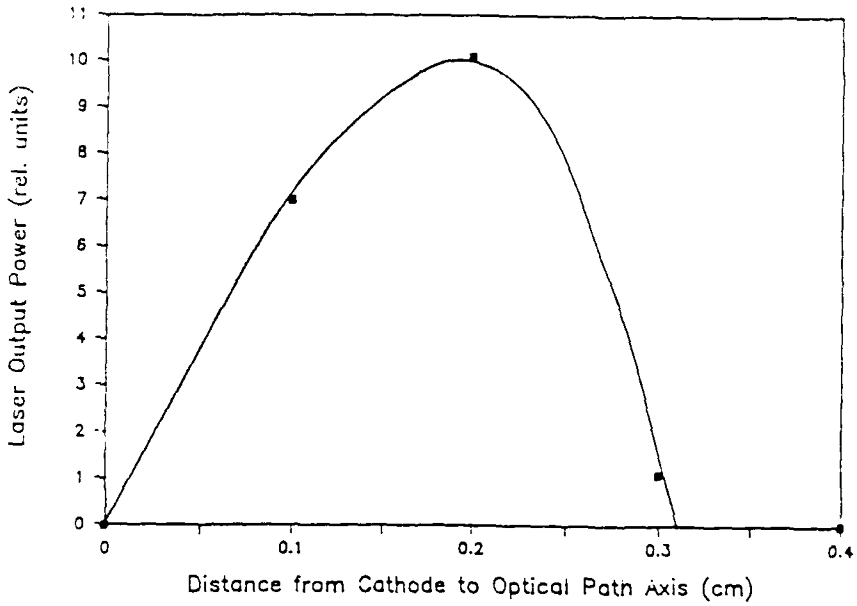

Figure 10: Laser output intensity of the 10738.7 SnII Penning excited laser transition as a function of distance between the cathode and optical path axis. Discharge current was 6 A with a pulsewidth of 27 µs. Gas flows were 1.3 liters per minute for Ar and 4 liters per minute for He. Two 2 mm diameter collimators were used.

As seen in figure 9, the metastable $He_M^*(2s\ ^3S_1)$ level of helium lies close to the laser upper level of the SnII laser transition. The Penning excitation process that is likely to contribute to the excitation of the SnII laser transition is

$$He_M^*(2s\ ^3S_1) + Sn(2p^2\ ^3P_0) \longrightarrow He(1s^2\ ^1S_0) + Sn^{+*}(5f\ ^2F_{5/2}^o) + e^- + \Delta E(0.11eV). \quad (4)$$

Penning reactions of the type of (4) have a high probability of occurrence ($\sigma \simeq 10^{-15}$ cm^2) [9]. Consequently, it is possible that a significant part of the laser excitation might occur through Penning collisions with helium metastables as in the case of PbII.

The SnII transition was unable to lase CW when a dc current of up to 0.8 A was applied to the slotted cathode. The discharge arced at larger currents before the threshold for CW laser action could be achieved. Laser action in tin was not observed in the 1.5 - 2.0 µm spectral region.

V. Recombination Lasing in Atomic Zinc and Enhanced Laser Intensity by Hydrogen Plasma Cooling:

Recombination lasing was also achieved in ZnI when the slotted cathode was made of zinc. The observed laser transition wavelength was 13152 ± 2 Å. This corresponds to a ZnI recombination laser transition previously reported by Wood II, Macklin and Silfvast [3], assigned to the 13151.42 Å line which had a level designation of $5p\ ^3P_1^o$ - $5s\ ^3S_1$.

For this laser transition to occur, the flows were adjusted to 1.3 liters per minute for Ar and 4 liters per minute for He. A partial Grotrian diagram displaying this laser transition is shown in figure 11.

The electron-ion recombination rate depends upon the electron temperature on the order of $T_e^{-9/2}$. Therefore, the cooler the plasma the higher the collisional recombination reaction rate making excitation through electron-ion recombination more efficient. The addition of hydrogen was observed to enhance the laser output intensity by cooling of the electron gas. This occurs because hydrogen molecules are lighter than helium atoms, are good conductors of heat, and will thermalize the electron gas to a lower temperature through more efficient elastic collisions. Consequently, the addition of H_2 can be expected to enhance the laser output which is in agreement with the observation.

Figure 12 shows the laser output intensity of the ZnI recombination laser transition as a function of the distance between the cathode and optical cavity axis. The relative laser intensity, both with and without the addition of hydrogen, is given. The gas flows in the discharge with hydrogen were 1.3 liters per minute for H_2, 1.3 liters per minute for Ar and 3 liters per minute for He. The addition of hydrogen causes the recombination reaction to be enhanced and laser action to occur closer to the cathode. Figure 13 illustrates the dramatic increase in laser output power obtained when H_2 is added to the discharge. This figure also shows how the time delay between the end of the current pulse and the beginning of the laser pulse shrinks

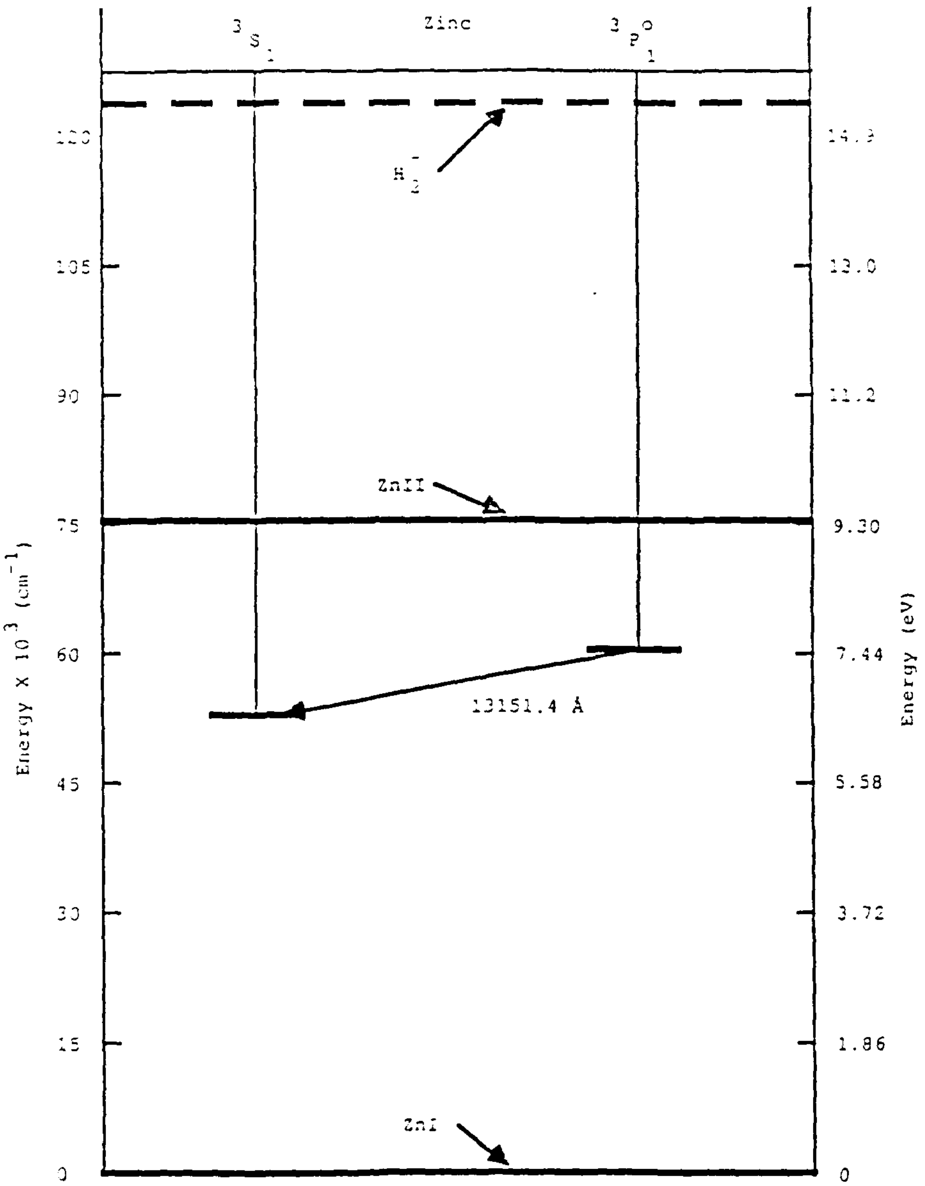

Figure 11: Partial Grotrian diagram of zinc.

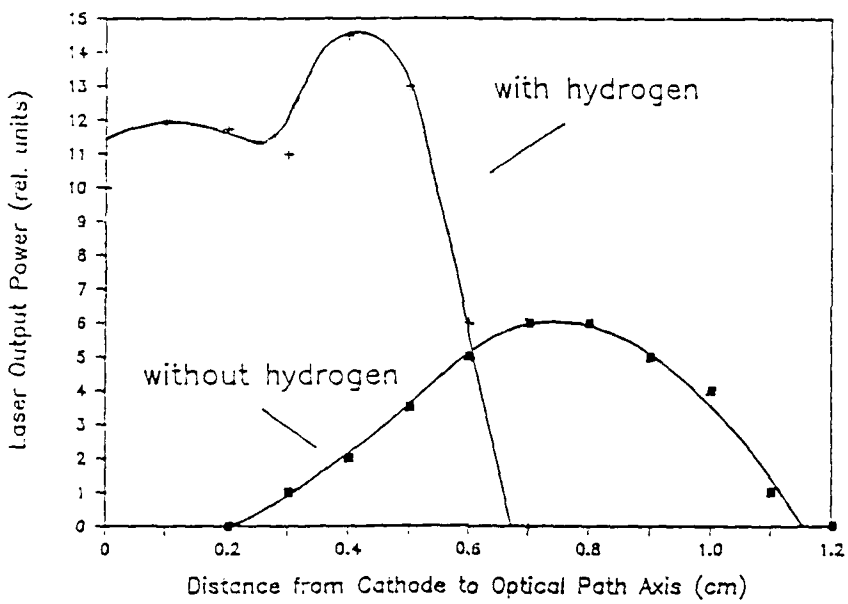

Figure 12: Laser output intensity of the 13151.4 Å ZnI recombination laser transition as a function of the distance between the cathode and optical cavity axis. Gas flows without H_2 were 1.2 liters per minute for Ar and 4 liters per minute for He. Gas flows with H_2 were 1.5 liters per minute for H_2, 1 liter per minute for Ar and 3 liters per minute for He. Discharge currents were 15 A with a pulsewidth of 10 µs. Two 2 mm diameter collimators were used.

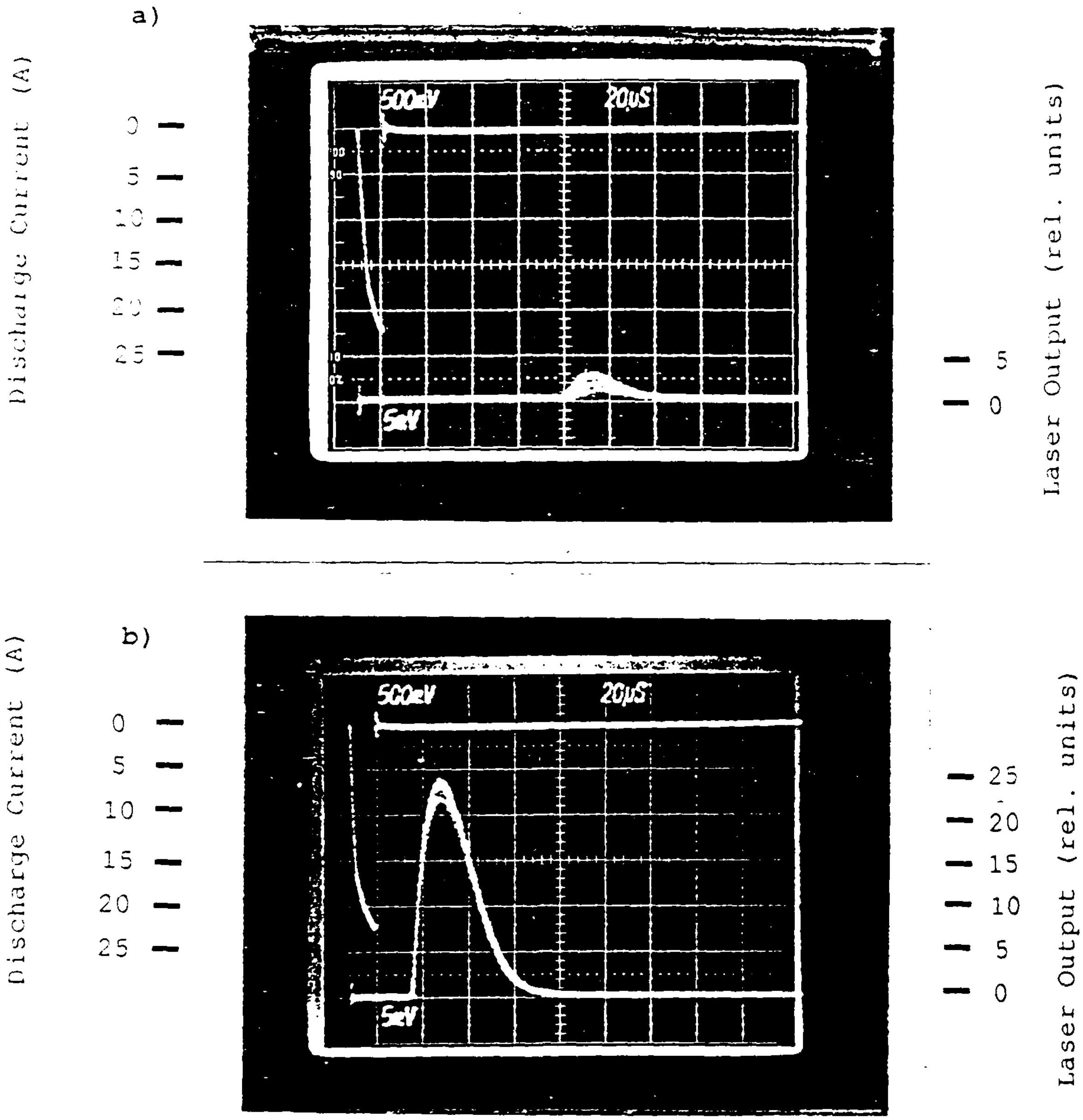

Figure 13: (a) Discharge current (upper trace) and laser output of the 13151.4 Å ZnI laser transition (lower trace) pulses without H_2. Gas flows were 1.3 liters per minute for Ar and 4 liters per minute for He. (b) Same as in part (a) but with the addition of H_2. Gas flows were 1.5 liters per minute for H_2, 1 liter per minute for Ar and 3 liters per minute He. The time delay decreased from 80 to 16 µs with the addition of H_2. The distance between the cathode and optical path axis was 0.5 cm.

with the addition of hydrogen. The laser output and the time delay between the end of the discharge current pulse and the beginning of the laser pulse as a function of current for both the inclusion and exclusion of hydrogen is given in figure 14. The addition of hydrogen to the plasma caused the laser output peak to increase, time delay to decrease and the value of the current corresponding to the laser output peak to increase. All of these phenomena can be attributed to an increase in the electron-ion recombination rate.

A dc input of up to 1.5 A was applied to the slotted zinc cathode. The ZnI recombination laser transition was not observed to lase in the CW mode regardless of the addition of hydrogen. Also, zinc did not lase in the 1.5 - 2.0 μm spectral region.

VI. Continuous Wave Recombination Lasing in ArI:

Recombination lasing in neutral argon was observed with slotted cathodes made of cast iron, tin or copper. The most detailed study of lasing in ArI was conducted using a cast iron cathode, and the results reported hereafter correspond to this case. The observed wavelength of the transition was 12704 ± 2 Å. The gas flow was 1.3 liters per minute of Ar and 4 liters per minute of He. This line was assigned to the ArI ($3d'$ $[3/2]_1^o$ - $4p'$ $[1/2]_1$) transition with an actual wavelength of 12702.2 Å [7]. A partial Grotrian diagram showing the ArI laser transition is given in figure 15. Solanki *et. al.* reported that pulse excitation of this laser transition caused by the contributions of both electron impact and recombination in the stationary (non-flowing)

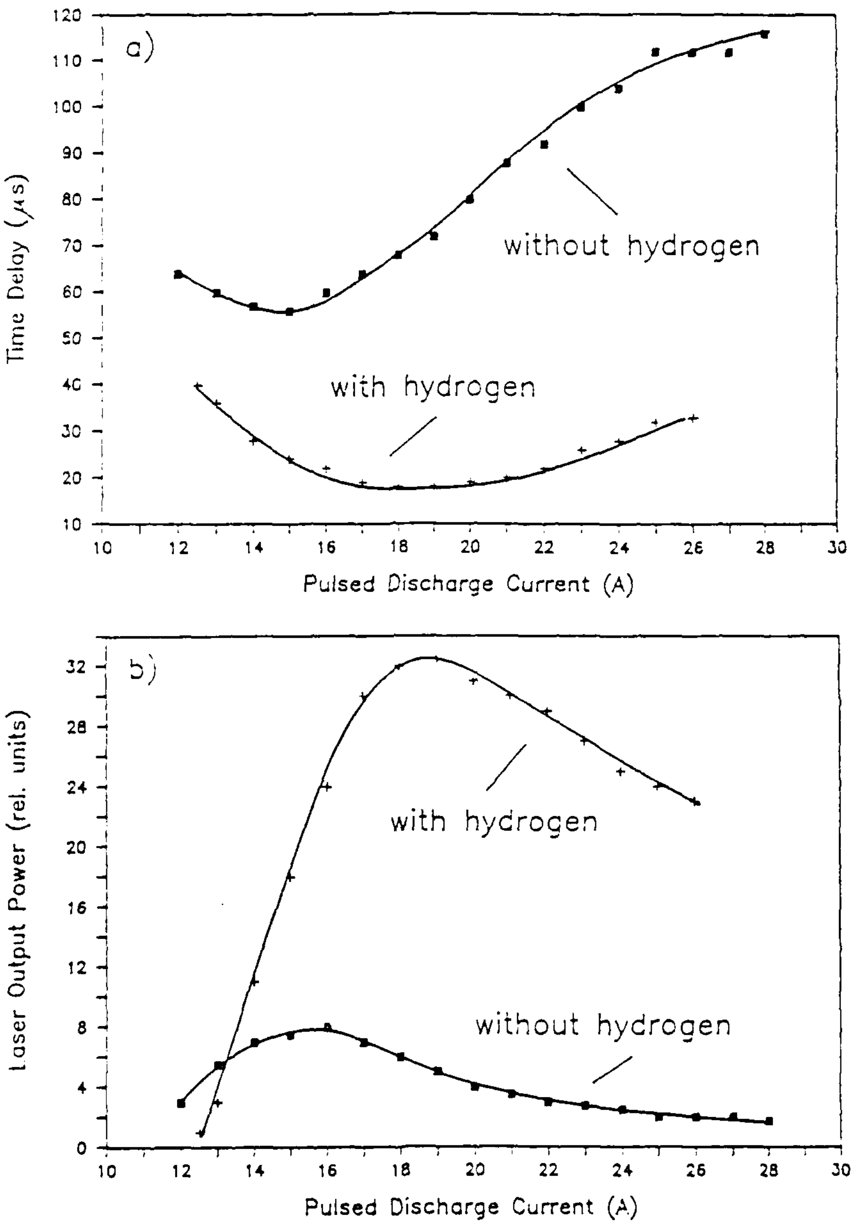

Figure 14: (a) Time delay and (b) laser output intensity of the 13151.4 Å ZnI laser transition as a function of the discharge current. Plots for both with and without hydrogen are given. Gas flows were the same as those in figure 4.13. Pulsewidth was 10 μs, and two 2 mm collimators were used. Distance from cathode to optical path axis without H_2 was 0.8 cm and with H_2 was 0.5 cm.

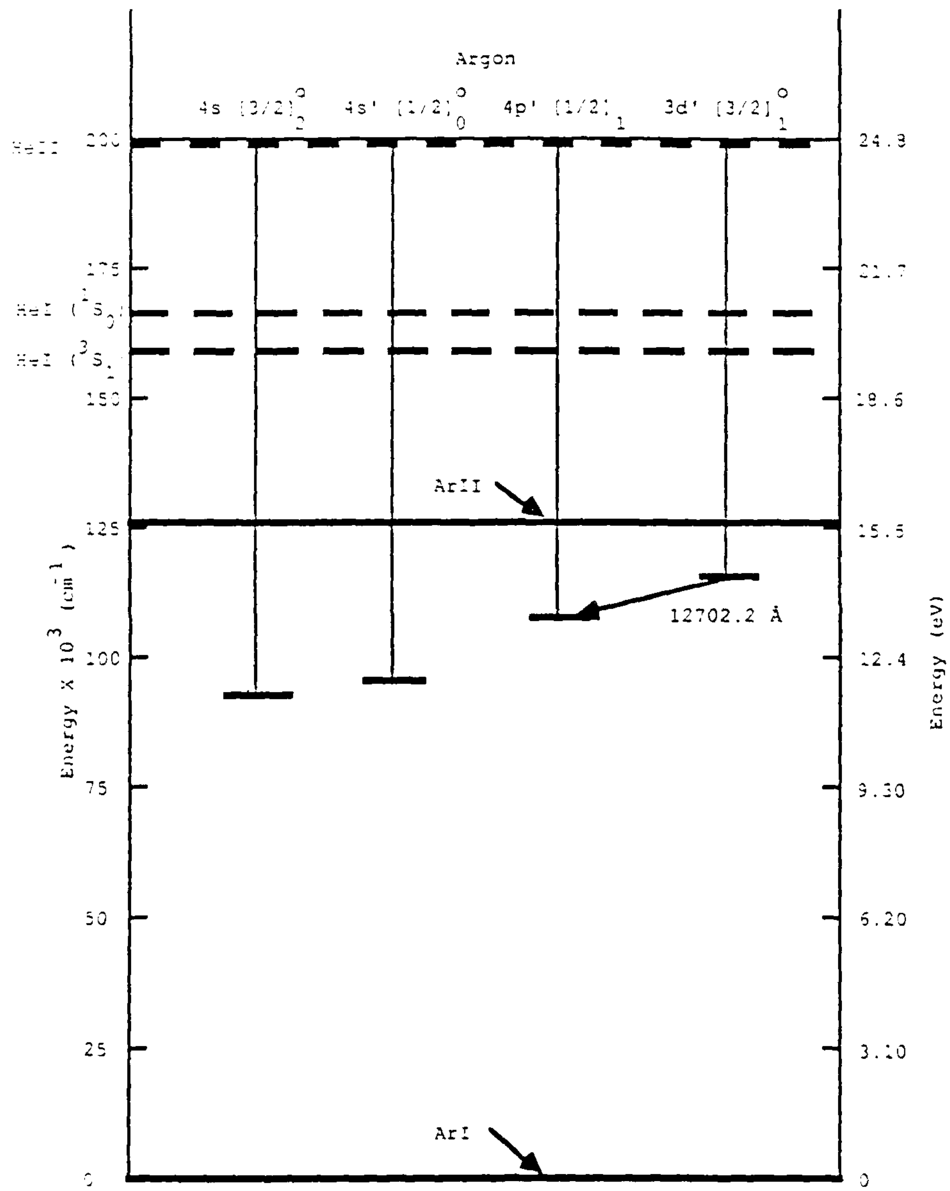

Figure 15: Partial Grotrian diagram of argon.

negative glow inside a hollow cathode slot [10]. Solanki *et. al.* also observed CW operation of this ArI laser line while using a hollow cathode device. They surmised that the CW mode of this transition was pumped via electron impact. This ArI laser transition has also been observed to be superradiant [11].

Figure 16 shows there are two peaks in the output intensity of the 12702.2 Å laser transition as a function of position of the axis of the optical cavity with respect to the cathode when the discharge was excited in the pulsed manner. The peak in the laser output intensity at 0.5 cm distant from the cathode is attributed to excitation following electron-ion recombination as in the case of the PbI and ZnI laser lines. The inversion in the region of the plume closer to the cathode is likely to receive a contribution from another excitation mechanism.

Figure 17 shows the laser output intensity and the time delay between the end of the current pulse and the beginning of the laser pulse as a function of the excitation current. The pulsewidth of the current pulse was 20 μs. Measurements were done at the cathode edge and at 0.5 cm from the cathode. As shown in this figure, the laser pulse time delay for the portion of the plasma at 0.5 cm from the cathode decreased when the input current was changed from the threshold value of 1.25 to 5 A. This time delay decrease corresponds to an increase in the laser output intensity also shown, and it is attributed to an increase in the electron-ion recombination rate due to a higher electron density. However, when the current is increased above 5 A, the electron density became excessive and the laser output decreased

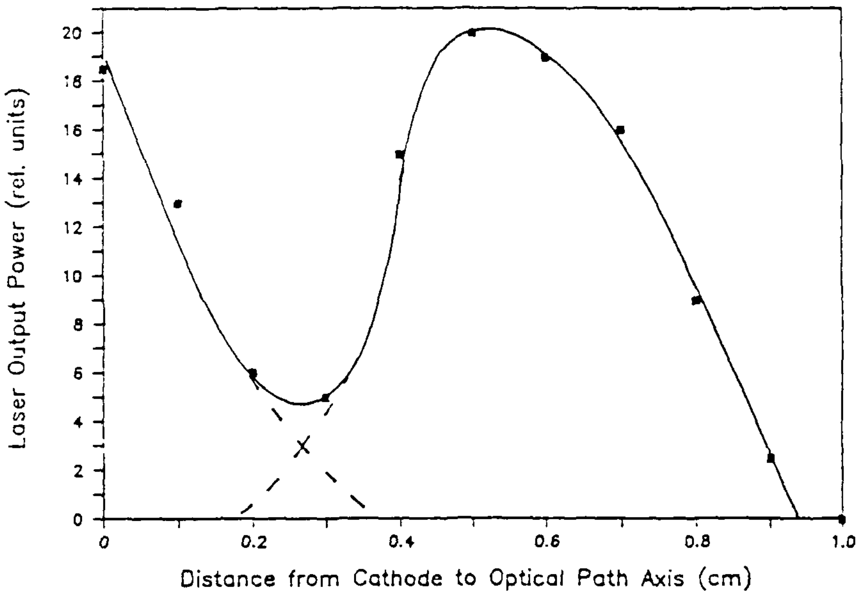

Figure 16: Laser output of the 12702.2 Å ArI laser transition as a function of discharge between the cathode and optical path axis. Discharge current was 7 A with a pulsewidth of 20 µs. Gas flows were 0.6 liters per minute for Ar and 5.5 liters per minute for He. Two 2 mm diameter collimators were employed.

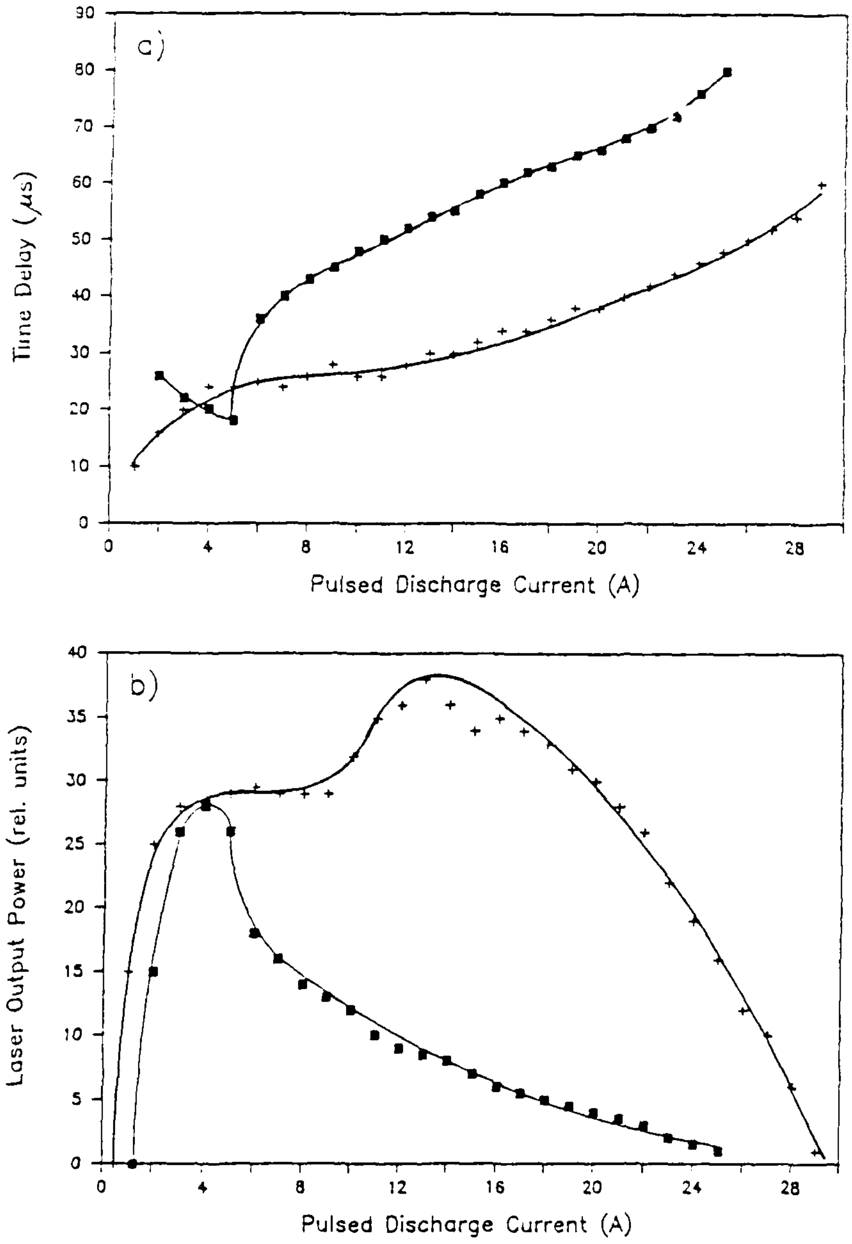

Figure 17: (a) Time delay and (b) laser output intensity of the 12702.2 Å ArI laser transition at 0.0 cm (+) and 0.5 cm (■) from the cathode as a function of discharge current. Current pulsewidths were 20 μs. Gas flows were 0.3 liters per minute for Ar and 5.5 liters per minute for He. Two 2 mm diameter collimators were employed.

while the time delay increased. The excessive electron density causes superelastic electron de-excitation of the laser upper level to begin dominating over the excitation processes.

The laser output intensity and time delay of the onset for laser action in the region of the flowing plasma near the cathode is also shown in figure 17. As can be seen, the time delay of the onset of the laser pulse after the end of the current pulse reaches 50 µs. Energetic electrons scattered out of the cathode slot could in principle contribute to the excitation in the region close to the cathode. However for this to be possible, electrons with enough energy to excite the transition are required to have lifetimes larger than the measured time delay of the laser pulse. The lifetime of a 300 eV electron was calculated for this purpose. To estimate a lower limit for the electron lifetime, one may assume that the most important type of collisions that the electron can initially go though are ionization and metastable creation of helium. The cross sections for these reactions ($\sigma \simeq 10^{-17}$ and 10^{-18} cm-2) are larger than any other cross sections for excitation from the ground state to any other excited level [12], and also the density of helium in the discharge is nearly 20 times that of argon. The calculated lifetime of a 300 eV electron for its energy to drop to a value too small to excite the laser upper level was calculated approximately to be of the order of tens of ns. Consequently, the observed 50 µs time delay is excessive for the electron impact reaction to aid electron-ion recombination in achieving a population inversion. Therefore, there must be another excitation mechanism to make laser action possible for this portion of the spatial laser output profile of figure 16.

Another type of reaction that needs to be investigated in relation with the excitation of the ArI transition is dissociative recombination. There are two possible dissociative recombination reactions. The first is dissociative recombination of $(HeAr)^+$. This ion is formed by:

$$He_M^*(2s\ ^3S_1) + Ar(3p^6\ ^1S_0) \longrightarrow (HeAr)^+ + e^- \tag{5}$$

and dissociative recombination of $(HeAr)^+$ occurs through reaction:

$$(HeAr)^+ + e^- \longrightarrow (HeAr)^* \longrightarrow He(1s^2\ ^1S_0) + Ar^* \tag{6}$$

where $(HeAr)^*$ is a short lived excited state in which the atoms are repulsed by each other and Ar^* is a high lying ArI level. The second possible dissociative recombination reaction is that of Ar_2^+. It is formed by:

$$Ar^+(3p^5\ ^2P_{3/2}^o) + 2Ar(3p^6\ ^1S_0) \longrightarrow Ar_2^+ + Ar(3p^6\ ^1S_0) \tag{7}$$

and by:

$$(HeAr)^+ + Ar(3p^6\ ^1S_0) \longrightarrow Ar_2^+ + He(1s^2\ ^1S_0) \tag{8}$$

and dissociative recombination of Ar_2^+ occurs through reaction:

$$Ar_2^+ + e^- \longrightarrow Ar_2^* \longrightarrow Ar^* + Ar(3p^6\ ^1S_0) \tag{11}$$

where Ar_2^* is an unstable excited molecule and Ar^* is a high lying level of ArI. Since the creation of the upper level was initiated from a reaction of a metastable state of He via (5) and (6) or the ground state of the argon or (HeAr) molecular ion via (7), (8) and (9), the lifetime for this creation rate of the laser upper level can be several tens of ns.

Previous investigators have found that reactions (5) and (6) have created population inversions in ArI with an upper level of 3d or 3d'' in the afterglow of the positive column of a glow discharge when the pressure of the helium-neon-argon mixture was > 50 Torr [13]. These investigators claimed that it was reactions (5) and (6) which created the inversion in argon since the addition of a minute amount of argon into the He-Ne laser device quenched the He-Ne laser output by depleting the $He_M^*(2s\ ^3S_1)$ population.

The pressure in the discharge chamber of the flowing hollow cathode system was measured to be 12 Torr when the gas flow through the hollow cathode was 6 liters per minute. Using this information, an estimation of the excitation rate into the laser upper level through both types of dissociative recombination was calculated using rate constants from [14] and [15]. The rate of (9) was calculated to be 100 times greater than the rate of (6). The pumping rate of (9) was estimated to be

$$dAr_u^*/dt_{(9)} \simeq 7\ 10^{15}\ cm^{-3}\ s^{-1}. \qquad (10)$$

This pumping rate is sufficient to generate a small signal gain of the order of 3.3 10^{-3} cm^{-1} which is compatible with the observation of laser action using totally reflecting mirrors. Therefore, the 12702.2 Å line of ArI near the cathode in the recombining plume might be excited by dissociative recombination of Ar_2^+ through (9).

Continuous wave laser action of the 12702.2 Å ArI laser transition was also observed when dc excitation was provided to the hollow cathode. A plot of the laser output intensity as a function of excitation current with the axis of the optical path 0.5 cm away from the cathode is shown in figure 18. Two, 2 mm collimators were used to differentiate emission origination from various regions of the discharge. The continuous wave laser action was observed to have a threshold current of 0.35 A, maximized at 0.47 A and ceased to lase at a current of 0.71 A. Figure 16 illustrates the variation of the laser output power as a function of position from the hollow cathode. The maximum laser intensity was observed to occur at 0.5 cm from the cathode and corresponds to the region of maximum excitation by electron-ion recombination in the pulsed experiments.

Another argon transition was also observed to lase in a pulsed manner at a measured wavelength of 12403 ± 2 Å. This transition is assigned to the ArI line with a wavelength of 12402.8 Å corresponding to the designation 3d $[3/2]_1^o$ - 4p $[3/2]_1$ [7]. This laser line was observed to lase when the gas flow was 1.1 liters per minute of Ar and 2.5 liters per minute of H_2 using a tin cathode. The excitation current was 10 A with a pulsewidth of 15 µs, and there was a distance of 0.1 cm between the cathode and optical cavity axis. While using the copper cathode, this transition lased when the gas flows were 1 liter per minute of Ar, 3 liters per minute of He and 1.5 liters per minute

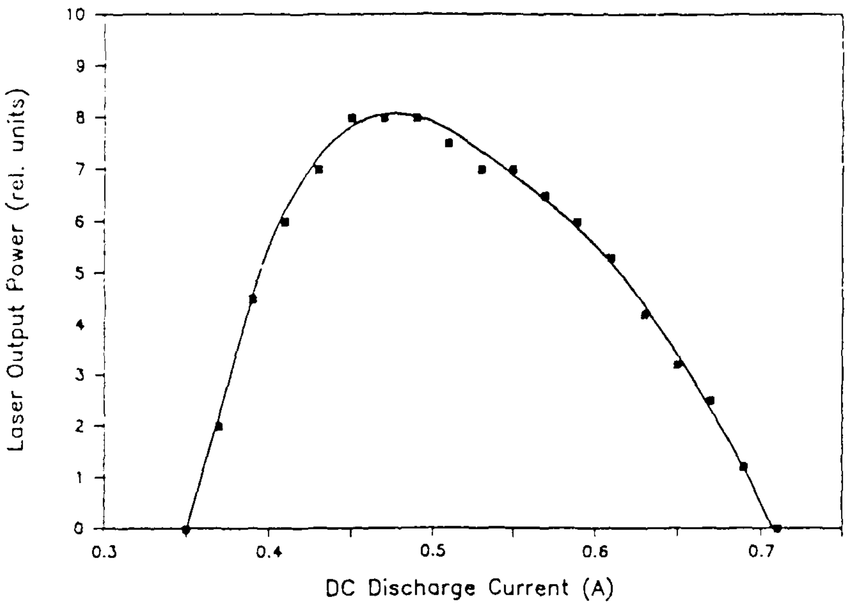

Figure 18: CW laser output of the 12702.2 Å ArI laser transition excited by electron-ion recombination as a function of discharge current. Distance from the cathode to the optical path axis was 0.5 cm. Gas flows were 0.3 liters per minute for Ar and 5.5 liters per minute for He.

of H_2. The excitation current was 35 A with a pulsewidth of 15 μs, and there was 0.5 cm between the cathode and optical cavity axis. No argon lines were observed to lase in the 1.5 - 2.0 μm spectral region.

VII. Other Observed Laser Transitions:

Laser oscillation in neon and molecular hydrogen was also observed. During the experiments with the tin cathode three NeI laser transitions were observed when the gas flows was adjusted to 1.5 liters per minute for Ne and 4 liter per minute for He. Neon was observed to oscillate at 11522 ± 2 Å. The actual wavelength for this transition is 11522.75 Å and corresponds to the transition 4s' $[1/2]_1^o$ - 3p' $[3/2]_2$ [7]. The excitation current was 6 A with a pulsewidth of 27 μs and 0.2 cm between the cathode and the optical cavity axis. The other two NeI laser transitions were observed when the gas flows in a Ne-H_2 mixture were 1.3 liters per minute for Ne and 1.3 liters per minute for H_2. The corresponding observed wavelengths were 11178 ± 2 and 11515 ± 2 Å with the actual wavelengths being 11177.5 and 11525.0 Å respectively [7]. The corresponding transition assignments for these laser lines are 4s' $[3/2]_2^o$ - 3p $[5/2]_3$ and 4s $[3/2]_1^o$ - 3p $[3/2]_1$ respectively. These two transitions were observed to lase when the discharge current was 15 A with a 15 μs pulsewidth and 0.2 cm between the cathode and the optical cavity axis.

During the experiments with the Zn cathode, molecular hydrogen was observed to lase at 13056 ± 2 Å. This was assigned to the wavelength of 13056.62 Å corresponding to a transition assignment of 2s $'\Sigma_g^+$ P(4)

$0 - 2p\ ^1\Sigma_u^+$ P(4) 1 [16]. This transition was observed to lase with the gas flows at 1.3 liters per minute for H_2, 1.1 liters per minute for Ar and 3 liters per minute for He. The input current was 15 A with a pulsewidth of 10 µs. Figure 19 shows the output intensity of the H_2 laser transition as a function of distance between the cathode and axis of the optical cavity.

VIII. Other Metal Vapor Afterglows:

Copper, iron and magnesium were also used for the slotted cathode to investigate possible infrared laser transitions. Pulsed currents reaching 35 A at pulsewidths ranging from 10 to 30 µs were employed for these cathodes. The distance between the cathode and optical cavity varied from 0.1 to 1.0 cm. None of these materials were observed to lase in the flowing hollow cathode laser system in either the 1.0 - 1.5 or the 1.5 - 2.0 µm spectral regions.

IX. Summary:

Laser oscillation in ten near-infrared laser transitions were obtained in a flowing negative glow plasma with 4 cm of gain medium optical path following the recombination of both singly and doubly charged ions. Table 1 summarizes the recombination laser transitions observed in the flowing hollow cathode plasma. The table lists the recombination excited transition wavelengths, the transitional assignments and the mode of operation. CW recombination laser

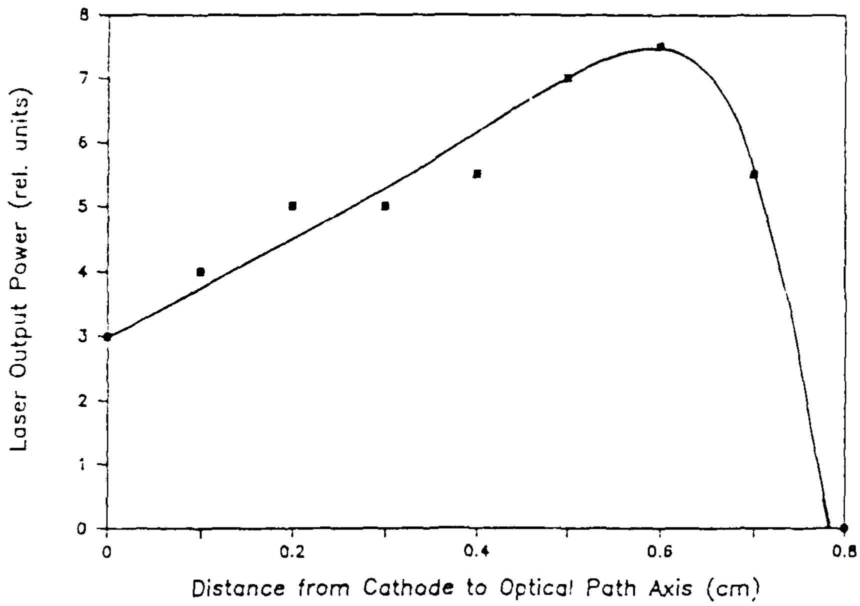

Figure 19: Laser output of the 13056.6 Å laser transition of H_2 as a function of the distance between the cathode and optical cavity axis. Discharge current was 20 A with a pulsewidth of 10 μs. Gas flows were the same as those of figure 4.10 with the addition of H_2. Two 2 mm diameter collimators were employed.

oscillation was obtained in argon. Four other electron-ion recombination laser transitions were observed in PbI, PbII, ZnI and SnII in a pulsed mode. The SnII laser transition is probably excited by both three-body electron-ion recombination and a Penning reaction with the He metastables. Table 2 shows other laser transitions observed, the actual transition wavelength and the conditions for laser actions. As shown for the case of laser oscillation in ZnI, the addition of hydrogen into the plasma cooled the plasma which, in turn, significantly increased the excitation of the laser upper level via electron-ion recombination.

Table 1

Observed Recombination Laser Transitions

Laser Medium	Wavelength	Transition Assignment	CW Laser Action Demonstration
ArI	12702.2 Å	$3d'[3/2]^{o}_{1} - 4p'[1/2]_{1}$	yes
PbI	13100.1 Å	$7p\ ^{3}P_{1} - 7s\ ^{3}P^{o}_{1}$	no
PbII	13216.9 Å	$6f\ ^{2}F^{o}_{7/2} - 7d\ ^{2}D_{5/2}$	no
ZnI	13151.4 Å	$5p\ ^{3}P^{o}_{1} - 5s\ ^{3}S_{1}$	no
SnII*	10743.3 Å	$5f\ ^{2}F^{o}_{5/2} - 6d\ ^{2}D_{3/2}$	no

* The SnII transition is also likely to be excited through Penning reactions with metastable helium atoms.

Table 2

Other Observed Laser Transitions

Laser Medium	Wavelength	Transition Assignment
ArI	12402.8 Å	$3d\ [3/2]^{o}_{1}$ – $4p\ [3/2]_{1}$
NeI	11522.8 Å	$4s'\ [1/2]^{o}_{1}$ – $3p'\ [3/2]_{2}$
NeI	11177.5 Å	$4s'\ [3/2]^{o}_{2}$ – $3p\ [5/2]_{3}$
NeI	11525.0 Å	$4s\ [3/2]^{o}_{1}$ – $3p\ [3/2]_{1}$
H_2	13056.6 Å	$2s\ {}^{1}\Sigma^{+}_{g}\ P(4)0$ – $2p\ {}^{1}\Sigma^{+}_{u}\ P(4)1$

References

1) J. J. Rocca, "CW Recombination Laser in a Flowing Negative Glow Plasma," *Appl. Phys. Lett.*, vol. 47, p. 1145, 1985.

2) C. Moore, "Atomic Energy Levels," vols I-III, Washington DC: U.S. GPO, 1949, 1952 and 1958.

3) O. R. Wood II, J. J. Macklin and W. T. Silfvast, "Neutral-Atom Recombination Lasers in CO_2 Laser-Vaporized Target Material," *IEEE J. Quantum Electron.*, vol. QE-21, p. 1714, Oct. 1985.

4) W. T. Silfvast, L. H. Szeto and O. R. Wood, II, "Simple Metal-Vapor Recombination Lasers Using Segmented Plasma Excitation," *Appl. Phys. Lett.*, vol. 36, p. 615, April 1980.

5) V. V. Zhukov, V. S. Kucherov, E. L. Latush and M. F. Sem, "Recombination Lasers Utilizing Vapors of Chemical Elements. II. Laser Action due to Transitions in Metal Ions," *Sov. J. Quantum Electron.*, vol. 7, p. 708, 1977.

6) J. M. Green and C. E. Webb, "The Production of Excited Metal Ions in Thermal Energy Charge Transfer and Penning Reactions," *J. Phys. B.*, vol. 7, p. 1698, 1974.

7) W. R. Bennett, Jr., "Atomic Gas Laser Transition Data: A Critical Review," IFI/Plenum, New York, 1980.

8) V. V. Zhukov, E. L. Latush, V. S. Mikhalevskii and M. F. Sem, "New Laser Transitions in the Spectrum of Tin and Population Inversion Mechanisms," *Sov. J. Quantum Electron.*, vol. 5, p. 468, 1975.

9) C. S. Willett, "Introduction to Gas Lasers: Population Inversion Mechanisms," Pergamon Press, New York, 1974.

10) R. Solanki, E. L. Latush, W. M. Fairbank, Jr. and G. J. Collins, "New Infrared Laser Transitions in Copper and Silver Hollow Cathode Discharges," *Appl. Phys. Lett.*, vol. 34, p. 568, 1979.

11) G. J. Linford, "High-Gain Neutral Laser Lines in Pulsed Noble-Gas Discharges," *IEEE J. Quantum Electron.*, vol. QE-8. p. 477, 1972.

12) J. J. Rocca, "CW Electron Beam Excited Metal Vapor Lasers," Doctoral Dissertation, Colorado State University, 1983.

13) E. I. Shtyrkov and E. V. Stubbes, *Optics Spectrosc.*, vol. 21, p. 143, 1966.

14) H. L. Kramer, J. A. Herce and E. E. Muschlitz, Jr., "Formation and Collisional Dissociation of Heteronuclear Rare-Gas Associative Ions," *J. Chem. Phys.*, vol. 56, p. 4166, 1972.

15) F. Kannari, A. Suda, M. Obara and T. Fujioka, "Theoretical Simulacion of Electron-Beam-Excited Xenon-Chloride (XeCl) Lasers," *IEEE J. Quantum Electron.*, vol. QE-19, p. 1587, 1983.

16) R. Beck, W. Englisch and K. Gurs, "Table of Laser Lines in Gases and Vapors," Springer-Verlag, New York, 1980.